

**Somatic mutations of *GNA11* and *GNAQ* in *CTNNB1*-mutant aldosterone-producing  
adenomas presenting in puberty, pregnancy or menopause**

Junhua Zhou<sup>1,2,27</sup>, Elena A. B. Azizan<sup>1,3,27\*</sup>, Claudia P. Cabrera<sup>2,4,27</sup>, Fabio Fernandes-Rosa<sup>5,27</sup>,  
Sheerazed Boulkroun<sup>5,27</sup>, Giulia Argentesi<sup>1,2</sup>, Emily Cottrell<sup>6</sup>, Laurence Amar<sup>5,7</sup>, Xilin Wu<sup>1,2</sup>, Sam  
O'Toole<sup>1,2</sup>, Emily Goodchild<sup>1,2</sup>, Alison Marker<sup>8</sup>, Russell Senanayake<sup>9</sup>, Sumedha Garg<sup>1,2,9</sup>, Tobias  
Åkerström<sup>10</sup>, Samuel Backman<sup>10</sup>, Suzanne Jordan<sup>11</sup>, Satyamaanasa Polubothu<sup>12</sup>, Dan Berney<sup>13</sup>, Anna  
Gluck<sup>14</sup>, Kate E. Lines<sup>14</sup>, Rajesh V. Thakker<sup>14</sup>, Antoinette Tuthill<sup>15</sup>, Caroline Joyce<sup>16</sup>, Juan Pablo Kaski<sup>17</sup>,  
Fiona Karet Frankl<sup>18</sup>, Lou Metherell<sup>6</sup>, Ada E. D. Teo<sup>19</sup>, Mark Gurnell<sup>9</sup>, Laila Parvanta<sup>20</sup>, William M.  
Drake<sup>21</sup>, Eva Wozniak<sup>22</sup>, David Klinzing<sup>23</sup>, Jyn Ling Kuan<sup>23</sup>, Zenia Tiang<sup>23,24</sup>, Celso E. Gomez Sanchez<sup>25</sup>,  
Per Hellman<sup>10</sup>, Roger Foo<sup>23</sup>, Charles A. Mein<sup>22</sup>, Veronica Kinsler<sup>11</sup>, Peyman Björklund<sup>10</sup>, Helen L.  
Storr<sup>6,28</sup>, Maria-Christina Zennaro<sup>5,26,28\*</sup>, and Morris J. Brown<sup>1,2,28\*</sup>

1. Endocrine Hypertension, Department of Clinical Pharmacology, William Harvey Research  
Institute, Queen Mary University of London, London, UK.
2. NIHR Barts Cardiovascular Biomedical Research Centre, Barts and The London School of  
Medicine and Dentistry, Queen Mary University of London, London, UK.

- 30 3. Department of Medicine, The National University of Malaysia (UKM) Medical Centre, Kuala  
31 Lumpur, Malaysia.
- 32 4. Centre for Translational Bioinformatics, William Harvey Research Institute, Queen Mary  
33 University of London, London, UK.
- 34 5. INSERM, U970, Paris Cardiovascular Research Center (PARCC), Paris, France.
- 35 6. Centre for Endocrinology, William Harvey Research Institute, Queen Mary University of London,  
36 London, UK.
- 37 7. Assistance Publique-Hôpitaux de Paris, Hôpital Européen Georges Pompidou, Unité  
38 Hypertension artérielle, Paris, France.
- 39 8. Department of Histopathology, Addenbrooke's Hospital, Cambridge, UK.
- 40 9. Metabolic Research Laboratories, Wellcome Trust-MRC Institute of Metabolic Science,  
41 Cambridge Biomedical Campus, Cambridge, UK.
- 42 10. Department of Surgical Sciences, Uppsala University, Uppsala, Sweden.
- 43 11. Cellular Pathology Department, Royal London Hospital, London, UK.
- 44 12. Genetics and Genomic Medicine, University College London Great Ormond Street Institute of  
45 Child Health, London, UK.
- 46 13. Department of Molecular Oncology, Barts Cancer Institute, Queen Mary University of London,  
47 London, UK.
- 48 14. Academic Endocrine Unit, Radcliffe Department of Medicine, University of Oxford, Oxford, UK.
- 49 15. Department of Endocrinology and Diabetes, Cork University Hospital, Cork, Ireland.
- 50 16. Clinical Biochemistry, Cork University Hospital, Cork, Ireland.
- 51 17. Centre for Inherited Cardiovascular Diseases, Great Ormond Street Hospital and University  
52 College London Institute of Cardiovascular Science, London, UK.
- 53 18. Cambridge Institute for Medical Research, University of Cambridge, Cambridge, UK.
- 54 19. Dept of Medicine, Yong Loo Lin School of Medicine, National University of Singapore, Singapore.
- 55 20. Department of Surgery, St Bartholomew's Hospital, London, UK.

- 56 21. Department of Endocrinology, St Bartholomew's Hospital, London, UK.
- 57 22. Barts and London Genome Centre, School of Medicine and Dentistry, Blizard Institute, Queen
- 58 Mary University of London, London, UK.
- 59 23. Cardiovascular Disease Translational Research Programme, Yong Loo Lin School of Medicine,
- 60 National University of Singapore, Singapore.
- 61 24. Genome Institute of Singapore, Agency for Science, Technology and Research, Singapore.
- 62 25. G.V. (Sonny) Montgomery VA Medical Center and Department of Pharmacology and Toxicology,
- 63 University of Mississippi Medical Center, Jackson, MS, USA.
- 64 26. Assistance Publique-Hôpitaux de Paris, Hôpital Européen Georges Pompidou, Service de
- 65 Génétique, Paris, France.
- 66 27. These authors contributed equally.
- 67 28. These authors jointly supervised this work.
- 68 \*email: [elena.azizan@ukm.edu.my](mailto:elena.azizan@ukm.edu.my); [maria-christina.zennaro@inserm.fr](mailto:maria-christina.zennaro@inserm.fr); [morris.brown@qmul.ac.uk](mailto:morris.brown@qmul.ac.uk)

69 Most aldosterone-producing adenomas (APA) have gain-of-function somatic mutations of ion-  
70 channels or transporters. However, their frequency in aldosterone-producing cell clusters of  
71 normal adrenals suggests a requirement for co-driver mutations in APAs. Here we identified gain-  
72 of-function mutations in both *CTNNB1* and *GNA11* by whole exome sequencing of 3/41 APAs.  
73 Further sequencing of known *CTNNB1*-mutant APAs led to a total of 16 of 27 (59%) with a somatic  
74 p.Gln209His, p.Gln209Pro or p.Gln209Leu mutation of *GNA11* or *GNAQ*. Solitary *GNA11* mutations  
75 were found in hyperplastic zona glomerulosa adjacent to double-mutant APAs. Nine of ten  
76 patients in our UK/Irish cohort presented in puberty, pregnancy, or menopause. Among multiple  
77 transcripts upregulated >10-fold in double-mutant APAs was *LHCGR*, the receptor for luteinizing or  
78 pregnancy hormone (human-chorionic-gonadotropin). Transfections of adrenocortical cells  
79 demonstrated additive effects of *GNA11* and *CTNNB1* mutations on aldosterone secretion and  
80 expression of genes upregulated in double-mutant APAs. In adrenal cortex, *GNA11/Q* mutations  
81 appear clinically silent without a co-driver mutation of *CTNNB1*.

82

83 Primary aldosteronism is a major cause of hypertension. This is potentially curable when due to an  
84 aldosterone-producing adenoma (APA) in one adrenal. Conversely, when primary aldosteronism is  
85 overlooked, it leads to resistant hypertension and high cardiovascular risk. The landmark report of  
86 somatic gain-of-function mutations in *KCNJ5* in 30-40% of APAs was followed by the discovery of  
87 further ion-channel or transporter mutations, mainly of *CACNA1D*, *ATP1A1* and *ATP2B3*, and of some  
88 clinical, pathological and biochemical differences between *KCNJ5*-mutant APAs and the others<sup>1-4</sup>. In  
89 particular, *KCNJ5*-mutant APAs are more common in women and have features resembling the  
90 cortisol-secreting cells of physiological zona fasciculata (ZF)<sup>5-8</sup>. Conversely, APAs with other ion-  
91 channel mutations are more common in men and resemble the physiological smaller aldosterone-  
92 producing cells of adrenal zona glomerulosa (ZG)<sup>4,9</sup>. Opinion has varied on whether the residual 20-  
93 30% of APAs without apparent mutation is due to sampling from parts of an APA that do not express

94 the aldosterone-synthesizing enzyme, CYP11B2, or to the existence of further somatic mutations yet  
95 to be discovered<sup>8-10</sup>. The genes whose mutation increases aldosterone production may differ from  
96 those responsible for tumor formation. Several of the former, particularly *CACNA1D*, are frequently  
97 mutated in the aldosterone-producing cell clusters (or nodules) of otherwise normal adrenals<sup>11</sup>.  
98 *KCNJ5* mutation was initially proposed to stimulate cell proliferation, as well as aldosterone  
99 production<sup>1</sup>, but the increased calcium entry consequent on mutation stimulates apoptosis rather  
100 than proliferation<sup>12</sup>. Wnt pathway-activating mutations of *CTNNB1*, encoding  $\beta$ -catenin, are found in  
101 ~5% of APAs.  $\beta$ -catenin is a co-activator for a number of transcription factors, and mutations that  
102 prevent phosphorylation of exon-3 residues are regarded as oncogenic in adrenal and other  
103 tumors<sup>8,10,13,14</sup>. However, there are only rare reports of *CTNNB1* mutations co-existing with somatic  
104 mutations that activate aldosterone production<sup>8,15</sup>, and in most APAs with *CTNNB1* mutations, these  
105 have been apparently solitary<sup>13,16</sup>. Whether *CTNNB1* mutations are able on their own to stimulate  
106 autonomous aldosterone production, or co-exist with other unidentified mutations, has not been  
107 resolved.

108         Three whole exome sequencing (WES) studies, which initially found *CACNA1D*, *ATP1A1*, and  
109 *ATP2B3* mutant APAs<sup>2-4</sup>, also reported several other genes mutated in the tumor DNA. However,  
110 even re-interrogation of the three WES studies together did not identify additional potential  
111 pathogenic mutations that are present in more than one sample. We therefore undertook another  
112 WES study of tumor and germline DNA from a new cohort of 41 APA patients in order to determine  
113 whether there are further genes with recurrent somatic mutation, and whether these were  
114 associated with a specific clinical or biochemical phenotype.

115

## 116 **Results**

**Identification of pathogenic somatic mutations in APAs.** WES identified somatic mutations of the four ion-channel/transporter genes at known hotspots in 29 of the 41 APAs (**Supplementary Table 1**). Somatic mutations of *CACNA1D* were the most frequent ( $n = 11$ ), followed by *KCNJ5* ( $n = 9$ ), *ATP1A1* ( $n = 5$ ) and *ATP2B3* ( $n = 4$ ). Three APAs had a known mutation of *CTNNB1*. All three were noted to have a second mutation of the Q209 residue of *GNA11*, which encodes the G-protein G11. This, or the closely homologous Gq, mediates the aldosterone response to its principal physiological stimulus, angiotensin II (**Fig. 1a**), and the highly conserved p.Gln209 residue is essential for GTPase activation (**Fig. 1b**)<sup>17,18</sup>. These mutations cause constitutive G11/q activation.

**Sanger sequencing and replication of *GNA11/Q* genotype.** *UK/Ireland (discovery cohort).* We identified p.Gln209His or p.Gln209Pro mutations of *GNA11* in the APAs of four further patients in whom presentation in periods of high LH/HCG had prompted discovery of somatic mutations in exon 3 of *CTNNB1* (**Supplementary Fig. 1a**). One patient was indeed our index case of *CTNNB1* mutation, detected by our first WES, where the p.Gln209His mutation of *GNA11* was reported in the pair-wise comparison analysis<sup>4</sup>. Once we recognized the co-existence of mutations in *CTNNB1* and *GNA11*, and associated features reported herein, targeted sequencing identified somatic exon 3 mutations of *CTNNB1* and p.Gln209 mutations of either *GNA11* or closely homologous *GNAQ* in three further APAs (**Supplementary Fig. 1a**). Of the total cohort, one was a 12-year old boy presenting at puberty, and the other nine were women, with presentations in early pregnancy ( $n = 7$ ) or menopause ( $n = 1$ ). All ten were completely cured of hypertension post-adrenalectomy (**Table 1**).

*French cohort.* We examined 13 APAs from patients in France for mutation at p.Gln209 of either *GNA11* or *GNAQ*. These APAs had previously undergone targeted sequencing and been found to have somatic mutations at exon 3 of *CTNNB1*. Of these 13 APAs, three had mutations at p.Gln209 of *GNA11* and one at p.Gln209 of *GNAQ* (**Table 2** and **Supplementary Fig. 1b**). During the study, double-mutation was suspected in a fifth woman, aged 17, whose primary aldosteronism dated from

puberty; her APA was confirmed to have somatic mutation at p.Gly34 of *CTNNB1* and p.Gln209 of *GNAQ* (**Table 2** and **Supplementary Fig. 1b**). As controls, we genotyped a further nine APAs with known ion-channel/transporter gene mutations but found no mutation of *CTNNB1*. In none of these nine cases was a mutation found in *GNA11* or *GNAQ*.

*Swedish cohort.* We achieved further replication by re-analyzing RNA-seq FASTQ data from the APAs of a published cohort of 15 Swedish patients<sup>19</sup>. This included three APAs with somatic mutations of *CTNNB1*. The re-analysis found one of these to have a p.Gln209His mutation of *GNAQ* (**Table 2**). No mutation of *GNA11* or *GNAQ* was seen in the other 12 APAs that had one of the known ion-channel/transporter gene mutations<sup>19</sup>.

In summary, 23/27 patients with *CTNNB1*-mutant APAs were women, and 16 of the 27 (59%) had a mutation at p.Gln209 of *GNA11* ( $n = 11$ ) or *GNAQ* ( $n = 5$ ). Among the latter, all were women except for the pubertal boy.

**Functional analyses in human adrenocortical cells.** H295R is an immortalized adrenocortical cell line heterozygous for the p.Ser45Pro mutation of *CTNNB1* but wild-type for *GNA11* (**Supplementary Fig. 2a**). Transfection of H295R cells by each of the *GNA11* mutations (**Supplementary Fig. 2b**) increased aldosterone secretion and *CYP11B2* expression (encoding aldosterone synthase) by 4.0-6.2-fold and 3.4-4.2-fold, respectively, compared to wild-type transfected cells (**Fig. 2a,b**). The stimulatory effect of angiotensin II 10 nM was retained in the mutant-transfected cells (**Supplementary Fig. 2c**). The stimulation of cortisol production by the mutations was less than of aldosterone (**Supplementary Fig. 2d,e**). In order to determine whether the Q209 mutations of *GNA11* stimulate aldosterone production, even in the absence of *CTNNB1* activation, the transfections of H295R cells were repeated after either silencing of *CTNNB1* using a Dharmacon SMARTpool siRNAs or 24-h treatment with the *CTNNB1* inhibitor ICG-001<sup>20,21</sup>. Both interventions reduced the aldosterone production relative to vehicle-treated cells, as anticipated by published experiments (**Fig. 2c,d**)<sup>22,23</sup>. However,

neither silencing of *CTNNB1* nor ICG-001 blunted the fold-increase in aldosterone secretion seen in mutant-transfected cells compared to wild-type (**Fig. 2c,d** and **Supplementary Fig. 2f**). As a further test of whether *GNA11* mutations require co-existing *CTNNB1* activation in order to increase aldosterone production, we used primary adrenocortical cells freshly dispersed from APAs with wild-type genotype for *CTNNB1* and *GNA11* (**Supplementary Table 2**). Cells were transfected with one each of the *CTNNB1* and *GNA11* mutants, or with both mutants together, and compared with cells transfected with vector or wild-type genes. Aldosterone secretion and CYP11B2 expression were increased by the individual mutations, but their combination caused substantially greater increases (**Fig. 2e** and **Supplementary Fig. 2g**). We also studied the p.Gln290His mutation of *GNAQ*. Its transfection into H295R cells increased aldosterone secretion by 1.93-fold (s.e.m. = 0.06) (**Fig. 2f**).

**Biochemical phenotype of APAs with double mutations. *LHCGR* expression.** We previously linked the presentation of the first three women at times of high circulating LH or HCG to high *LHCGR* expression by *CTNNB1*-mutant APAs<sup>16</sup>. To determine whether the association requires double-mutation of *CTNNB1* and *GNA11*, rather than *CTNNB1* mutation alone, we performed qPCR of *LHCGR* in all *CTNNB1*-mutant APAs from the three cohorts. Fold-changes >10 (compared to available controls for each cohort) were seen in 15/16 double-mutant APAs (**Fig. 3a-c**). The exception, patient 10, was the sole patient with a p.Gln209Leu mutation. Of possible note, her adrenalectomy coincided with menstruation, when *LHCGR* expression, at least in ovarian follicles, is suppressed to <10% of maximum<sup>24</sup>. Conversely, 7/9 single-mutant APAs had low or undetectable *LHCGR* mRNA ( $P = 0.0001$ , Fisher exact test).

APAs from the ten UK/Irish patients were positive for *LHCGR* on immunohistochemistry (IHC) (**Fig. 3d** and **Supplementary Fig. 3a**). Expression within APAs was variable, particularly in APAs with variable expression of CYP11B2. In the APA from patient 10, which had low mRNA expression for *LHCGR*, the protein was concentrated in a visually distinct segment; this allowed demonstration that



variation in IHC signal corresponded to fold-change on qPCR (**Supplementary Fig. 3a**). Adrenal medulla was also unexpectedly positive, confirmed by analyses of laser-capture microdissected RNA (**Supplementary Fig. 3b**). Since LHCGR in steroidogenic cells is coupled to both G $\alpha$ S and G $\alpha$ Q/11, the consequences of activation will depend not only on LH/HCG levels, but also on downstream signalling, and paracrine stimulation by other cell types with physiological expression of LHCGR<sup>25</sup>. There was also striking heterogeneity in subcellular sites of expression (**Supplementary Fig. 3c**). Membranous and vesicular expression were most common in double-mutant APAs, but cytosolic in adjacent ZG (**Supplementary Fig. 3d**).

There is no expression of LHCGR in H295R cells, indicating that LH/HCG stimulation is not essential in these cells to the induction of autonomous aldosterone production by *GNA11/Q* mutation (**Fig. 2a-b,f** and **Supplementary Fig. 3e**). The steroidome of H295R cells suggests a cell of origin in zona reticularis, far downstream of the primordial adrenogenital cells that are the common precursor of gonads and adrenal cortex<sup>26</sup>. We therefore turned again to primary adrenocortical cells, comparing LHCGR expression in cells transfected with mutant *GNA11* and *CTNNB1*, alone or together. qPCR showed greater expression of *LHCGR* in cells transfected with mutations of both genes, than with single-mutations or vector (**Fig. 3e**). The low transfection of primary cells also enabled comparisons of individual cells, by immunofluorescence, both within and between each well. The red immunofluorescence for LHCGR was qualitatively intense, and frequently membranous, in cells positive for both mutations, but was scarce in GFP-negative cells lacking *GNA11* p.Gln209 mutation (**Fig. 3f** and **Supplementary Fig. 3e-i**). Quantitative analysis confirmed a higher LHCGR intensity in cells with *GNA11*-mutant transfection (**Fig. 3g**). However some *GNA11*-mutant cells were LHCGR positive even without *CTNNB1* transfection. Post-hoc analysis showed that LHCGR (red) intensity was qualitatively and quantitatively associated with immunofluorescence (magenta) for *CTNNB1* (**Supplementary Fig. 3j**), consistent with adrenocortical Wnt activation in primary aldosteronism<sup>27,28</sup>. When both plasmids were transfected into primary adrenocortical cells, and these were compared by intensity of green (*GNA11*) and magenta (*CTNNB1*), the red (LHCGR)

intensity was 31-144 fold higher in cells with GNA11-p.Gln209Pro transfection and high CTNNB1 intensity than in other cells (**Extended Data Fig. 1**).

*Expression of top differentiated genes.* *LHCGR* was the most upregulated gene (compared to other APAs in the same microarray)<sup>16</sup> in the APA of patient 4, but a weaker pregnancy association in the replication cohorts (**Tables 1 and 2**) prompted us to ask whether there are other genes consistently upregulated in the double-mutant APAs. We re-examined our previous public-domain expression data (microarray or RNA-seq) performed in three of the double-mutant APAs before their genotype was known: the index case from 2013 (patient 4)<sup>4,29,30</sup>, the APA from a menopausal woman (patient 6)<sup>5</sup>, and the newly diagnosed Swedish double-mutant APA (S1)<sup>19</sup>. Unsupervised hierarchical clustering analysis of the most variably expressed genes in the three studies showed clustering of the three double-mutant APAs, and a high proportion of genes were many-fold upregulated compared to other APAs (**Fig. 4a**). *LHCGR* is among several ‘hallmark’ genes with uniquely high expression in the three double-mutant APAs, including the neuronal cell adhesion molecule *TMEM132E* and the Wnt inhibitor *DKK1* (**Fig. 4b**). Further genes are also upregulated in other ZG-like (compared to *KCNJ5*-mutant) APAs, or in one or both solitary *CTNNB1*-mutant APAs. A small number of genes are downregulated in the double-mutant APAs, including *CYP11B1* (**Fig. 4b**). This gene encodes the final enzyme in cortisol synthesis (11  $\beta$ -hydroxylase). Enrichment analysis using DAVID (Database for Annotation, Visualization and Integrated Discovery v6.8) showed significant enrichment of features or terms concerned with cell-junction/cell adhesion or synapse (**Supplementary Table 3**).

qPCR confirmed large (10’s to 1000’s-fold) higher expression of several of the hallmark transcripts in 4-5 double-mutants (from whom RNA of fresh-frozen tissue remained) than in nine APAs without mutations of either gene (**Fig. 4c,d**) or (for *TMEM132E*) than in seven APAs with solitary mutation of *CTNNB1* (**Fig. 4e**). However, in H295R cells that were transfected with mutant *GNA11* and that have germline S45P mutation of *CTNNB1*, *TMEM132E* was the only one of the six

tested genes to be significantly and substantially upregulated (**Fig. 4f**). *TMEM132E* and *LHCGR* were the top genes that differed most robustly between double-mutant and other APAs, including those with solitary mutations of *CTNNB1* (**Fig. 4e** and **Supplementary Fig. 4**). *LHCGR* itself remained undetectable after transfection of mutant *GNA11*.

In a previous IHC analysis of eight *CTNNB1*-mutant APAs, we reported four with low CYP11B2 (H-score < 30) and high CYP11B1 expression (H-score > 200) versus three with high CYP11B2 (H-score > 200) and low CYP11B1 expression (H-score < 1)<sup>13</sup>. No genotyping was available from these patients, but IHC in two of the current Swedish cohort showed similar contrast between the single- and double-mutant APAs (**Supplementary Fig. 5a**), supported by qPCR and aldosterone measurements (**Supplementary Fig. 5b**). These findings, and the low *CYP11B1* expression highlighted in the heatmap of the three double-mutant APAs (**Fig. 4b**), prompted us to analyze *CYP11B1* and *CYP11B2* expression in double-mutant APAs compared to APAs with single mutations of *CTNNB1* or other genotypes. qPCR confirmed a low *CYP11B1*:*CYP11B2* ratio, and an overall low expression of *CYP11B1*, in ten double-mutant APAs with available RNA (**Fig. 5a**). IHC of all the UK/Irish double-mutant APAs showed absent CYP11B1 but strong staining of CYP11B2 (**Fig. 5b**).

**Phenotype and genotype of adjacent adrenals.** The IHC also showed consistent hyperplasia of adjacent ZG, with absence of both CYP11B1 and CYP11B2 staining, but weak/moderate staining for *LHCGR* (**Supplementary Fig. 5c**). There were few aldosterone-producing cell clusters (APCCs), and a possible atrophy of zona fasciculata (ZF). The ZG expansion resembles that in mice with transgenic activation of adrenal Gq or *CTNNB1*<sup>31,32</sup>. A similar picture is also seen in a minority of patients with mosaicism of *GNAS* at the residues analogous to the p.Gln209 or p.Arg183 residues of *GNA11*/Q (McCune-Albright syndrome)<sup>33-35</sup>. We therefore wondered whether loci of *GNA11* mutation may be present in the adrenal cortex adjacent to APAs with *GNA11* mutations at p.Gln209.

267 Multiple punch biopsies were taken for genomic DNA ( $\pm$  cDNA sequencing and qPCR) from  
 268 six regions of fresh-frozen adrenal available from patient 7 (**Fig. 6a-c**). Genomic DNA from three  
 269 regions had the same double-mutation genotype as the original tumor (**Supplementary Fig. 6a**); in  
 270 one case, the associated cDNA had low expression of *CYP11B2* and *LHCGR* (**Fig. 6b**). Samples from  
 271 the other three regions were *CTNNB1* wild-type, but one (DNA1) had the same p.Gln209His  
 272 mutation of *GNA11* as the APA, homozygous in R1 genomic DNA and heterozygous in R1 cDNA  
 273 (**Supplementary Fig. 6a** and **Fig. 6c**). The latter had undetectable levels of *CYP11B2*, *LHCGR* (**Fig. 6b**)  
 274 and other hallmark differentially expressed genes (DEG) high in double-mutant APAs  
 275 (**Supplementary Fig. 6a**), confirming its separation from the APA. In patient 6, a focal area of peri-  
 276 medullary ZG cells was weakly positive for CYP11B2 (**Extended Data Fig. 2a**) and for mutations of  
 277 *GNA11* and *CTNNB1* (**Extended Data Fig. 2b,c**). qPCR from this double-mutant region showed  
 278 intermediate expression of several DEG genes (**Extended Data Fig. 2d**). For more precise analysis and  
 279 location, we undertook laser capture microdissection (LCM) of a formalin-fixed paraffin embedded  
 280 adrenal section from patient 1, in which ZG was intact in the adjacent adrenal gland (**Fig. 6d,e**). Two  
 281 of eight sites (ZG1 and ZG6) at distinct ends of the adrenal limbs were, respectively, heterozygous or  
 282 homozygous for the same p.Gln209Pro mutation in *GNA11* as the APA, but did not have the APA's  
 283 mutation of *CTNNB1* (**Fig. 6f** and **Supplementary Fig. 6b**). The findings of APA mutations in adjacent  
 284 adrenal were replicated in each case by up to three quantitative techniques (ddPCR for *GNA11* and  
 285 *GNAQ*, targeted NGS for both tumor genes, and WES) (**Supplementary Table 4a-d**). There was high  
 286 concordance between ddPCR, NGS and Sanger sequencing when analyzed in the same sample, e.g.  
 287 in patient 6 (**Extended Data Fig. 2b,c** and **Supplementary Table 4a**). Where fresh samples were re-  
 288 taken, concordance with Sanger sequencing was lower, e.g. patient 1 (**Fig. 6d-f** and **Supplementary**  
 289 **Table 4b**) and patient 7 (**Supplementary Table 4a,b**), and NGS detected both tumor genes in some  
 290 samples. Minor allele frequencies (MAF) > 3% were not seen for other bases in the targeted region  
 291 or at the same base in other adrenals. No mutations were found in four adrenals adjacent to APAs

with *KCNJ5* or *CACNA1D* mutations (**Supplementary Table 4d**), nor in a limited number of scrapings adjacent to the double-mutant APAs from patients 2, 8, and 9 (**Supplementary Table 4b,c**).

In McCune-Albright syndrome, *GNAS* mutation can be difficult to detect, and appear homozygous, heterozygous or absent at adjacent sites<sup>36,37</sup>. Finding an APA's mutation at disparate sites of adjacent ZG could point to an origin during adrenogenesis, but strictly defined mosaicism is hard to prove within single tissues.

## Discussion

We report the discovery of gain-of-function mutations of the G-protein gene *GNA11*, or its close homolog *GNAQ*, in multiple APAs. To date, the mutation is always residue p.Gln209 and associated with a gain-of-function mutation of *CTNNB1*. Mutation of p.Gln209, or homologous p.Gln in *GNAS* or *GNA12-14*, impair hydrogen bonds between G-protein  $\alpha$  and  $\beta$  subunits<sup>17,18</sup>. In ZG, Gq/11 mediate the aldosterone response to angiotensin II via stimulation of intracellular  $\text{Ca}^{2+}$  release by inositol trisphosphate (IP3)<sup>38</sup>. Somatic mutations of the Gln209 or Arg183 codons of *GNA11* or *GNAQ* have been reported in the majority of uveal melanomas and in several congenital skin or vascular lesions, including blue nevi and Sturge-Weber syndrome<sup>39-41</sup>. In some congenital lesions, the mutation of *GNA11/Q* is mosaic, being found in several disparate sites<sup>42</sup>.

The role of Wnt signalling in adrenal development and APA formation is well established<sup>28,43,44</sup>. Usually the Wnt activation in APAs is present without mutation of *CTNNB1*, but gain-of-function somatic mutations of exon 3 of *CTNNB1* are found in ~5% of APAs, as well as other adrenal tumors<sup>10,13,14,27,45,46</sup>. 20-30% of malignant adrenocarcinomas of the adrenal (ACC) have the same mutations of *CTNNB1* as occur in APAs<sup>27</sup>, but mutations of *GNA11/Q* are absent from ACCs, and their common co-driver mutations are in different genes (e.g. *TP53*, *MED12*)<sup>47</sup>. In many malignancies, co-drivers are the exception, often following chemotherapy<sup>48,49</sup>.

316           So why do these two well known oncogenic mutations cluster in APAs, but seemingly no  
317 other tumor? Occasional APAs have been reported with dual mutation of *CTNNB1* and *CACNA1D*<sup>50</sup>.  
318 However, unlike *GNA11/Q*, *CACNA1D* appears to be the sole driver in most APAs where it is  
319 mutated, or to co-exist with such a variety of mutations that no other gene was recurrently co-  
320 mutated in our 11 *CACNA1D*-mutant APAs. The greater prevalence of *CTNNB1* than *GNA11/Q*  
321 mutations, and the ZG hyperplasia of mice with *CTNNB1* mutations, might suggest that *GNA11/Q*  
322 mutations arise in a subset of *CTNNB1*-mutant APAs<sup>51</sup>. In possible support, Wnt activation by  
323 germline mutation of *APC* predisposes, rarely, to somatic mutation of *KCNJ5*<sup>52</sup>. In possible opposition  
324 is the high CYP11B1 expression of solitary *CTNNB1*-mutant APAs, but exceptionally low expression in  
325 the double-mutants, suggesting different sites of origin within the adrenal cortex.

326           The clue to whether one mutation generally precedes the other may come from growing  
327 evidence that increased transcription drives mutation<sup>53</sup>, and from examples where Gq/11 lie  
328 upstream of *CTNNB1* activation. As proof-of-concept, mutation of upstream *MAPK* in the  
329 melanogenesis pathway leads via second-hit mutation of *CTNNB1* to penetrating nevi<sup>54</sup>. A recent  
330 study of p.Gln209 mutations of *GNAQ* in uveal melanoma suggested that these cause hyperplasia,  
331 ‘being insufficient for neoplastic transformation’, and highlighted clustering of driver mutations  
332 within KEGG pathways to explain recurrent second hits<sup>55</sup>. Coincidentally, *GNA11/Q* and *CTNNB1*  
333 feature together in just one KEGG pathway, melanogenesis. Adrenal MC1R expression, and presence  
334 of melanin in occasional pigmented adrenal nodules, seems unlikely to be directly relevant to our  
335 double-mutant APAs<sup>56,57</sup>, but the connection between *GNAQ* and *CTNNB1* in melanogenesis is the  
336 Wnt receptor FZD6, which is the most upregulated Frizzled in ZG<sup>29</sup>. An additional potential link  
337 between Gq/11 and *CTNNB1* activation is through *RSPO3*<sup>58</sup>. The *RSPO3*-*LGR5* pathway is active in ZG,  
338 maybe controlling cell proliferation and migration as in intestinal crypts<sup>29,59-61</sup>. In summary, *GNA11/Q*  
339 mutations may arise early and create conditions in which a second hit in *CTNNB1* leads to APA  
340 formation. Proven examples of *GNA11/Q* mosaicism, and the disconnected, discrete areas of *GNA11*  
341 mutation in adjacent hyperplastic ZG, are consistent with this view<sup>42</sup>. *CTNNB1* mosaicism has

occasionally been suggested, and much further work is required to determine whether mosaicism for either or both genes might be the antecedent to double-mutant APAs<sup>62,63</sup>. A case of *KCNJ5* mosaicism was recently reported<sup>64</sup>.

In the replication cohorts from France and Sweden, single-mutant outnumbered double-mutant APAs by 2:1, whereas no single-mutant APAs were found among UK patients. The latter came from a variety of endocrine, renal and hypertension clinics, with no apparent referral bias. Ethnic variation in somatic mutation of several genes is recognized in APAs, with *KCNJ5* mutations being more common in cohorts of East Asian ancestry than those of European ancestry, and less frequent than *CACNA1D* in patients of African ancestry, in whom no *CTNNB1* mutations are yet reported<sup>50,65</sup>. Ancestral variation within Europe may seem less likely than between continents. Although melanogenesis is probably irrelevant to adrenal p.Gln209 mutation, *MC1R* genotype and phenotype (red hair) illustrate intra-continental heterogeneity<sup>66</sup>.

Our findings suggest that onset of hypertension in the first trimester – the period of peak HCG secretion – should prompt consideration of primary aldosteronism. Most pregnancy-associated hypertension arises in later trimesters. The index case of our original report was successfully managed on amiloride through pregnancy, whereas undiagnosed primary aldosteronism is high-risk for mother and fetus<sup>16,67</sup>. We previously linked the seemingly explosive presentation of *CTNNB1*-mutant APAs in early pregnancy to their induction of LHCGR expression. We have not ourselves confirmed LH responsiveness of cells transfected with mutant *CTNNB1* and *GNA11*, but LH can induce the *CYP11B2* promoter by 25-fold in adrenocortical cells transfected with LHCGR expression<sup>16,68</sup>. LH stimulates modest increases in aldosterone secretion in some patients with primary aldosteronism, and LHCGR is indeed commonly expressed in APAs and adjacent adrenal – though at a much lower level than in our *CTNNB1*-mutant APAs presenting in pregnancy<sup>16,69,70</sup>. Subsequently, it became apparent that *CTNNB1* mutation was usually insufficient to cause the phenotype of LH/HCG-dependent primary aldosteronism<sup>69,71,72</sup>. Our finding of a second driver

367 mutation explains much of the discrepant experience. Although the APA transcriptomes, and  
368 transfections of primary cells, show some overlap between phenotypes of single- and double-  
369 mutation, we infer that a double-hit within related pathways is more likely than a single-hit to cause  
370 large increases in expression of *LHCGR* and of other genes that may influence clinical presentation.



## 371    **References**

- 372    1.     Choi, M. et al. K<sup>+</sup> channel mutations in adrenal aldosterone-producing adenomas and  
373       hereditary hypertension. *Science* **331**, 768-772 (2011).
- 374    2.     Beuschlein, F. et al. Somatic mutations in *ATP1A1* and *ATP2B3* lead to aldosterone-producing  
375       adenomas and secondary hypertension. *Nat. Genet.* **45**, 440-444 (2013).
- 376    3.     Scholl, U. I. et al. Somatic and germline *CACNA1D* calcium channel mutations in aldosterone-  
377       producing adenomas and primary aldosteronism. *Nat. Genet.* **45**, 1050-1054 (2013).
- 378    4.     Azizan, E. A. et al. Somatic mutations in *ATP1A1* and *CACNA1D* underlie a common subtype  
379       of adrenal hypertension. *Nat. Genet.* **45**, 1055-1060 (2013).
- 380    5.     Azizan, E. A. et al. Microarray, qPCR and *KCNJ5* sequencing of aldosterone-producing  
381       adenomas reveal differences in genotype and phenotype between zona glomerulosa- and  
382       zona fasciculata-like tumors. *J. Clin. Endocrinol. Metab.* **97**, E819-E829 (2012).
- 383    6.     Monticone, S. et al. Immunohistochemical, genetic and clinical characterization of sporadic  
384       aldosterone-producing adenomas. *Mol. Cell. Endocrinol.* **411**, 146-154 (2015).
- 385    7.     Akerstrom, T. et al. Novel somatic mutations and distinct molecular signature in  
386       aldosterone-producing adenomas. *Endocr. Relat. Cancer* **22**, 735-744 (2015).
- 387    8.     De Sousa, K. et al. Genetic, cellular, and molecular heterogeneity in adrenals with  
388       aldosterone-producing adenoma. *Hypertension* **75**, 1034-1044 (2020).
- 389    9.     Nanba, K. et al. Targeted molecular characterization of aldosterone-producing adenomas in  
390       White Americans. *J. Clin. Endocrinol. Metab.* **103**, 3869-3876 (2018).
- 391    10.    Wu, V. C. et al. The prevalence of *CTNNB1* mutations in primary aldosteronism and  
392       consequences for clinical outcomes. *Sci. Rep.* **7**, 39121 (2017).
- 393    11.    Nishimoto, K. et al. Aldosterone-stimulating somatic gene mutations are common in normal  
394       adrenal glands. *Proc. Natl. Acad. Sci. USA* **112**, E4591-E4599 (2015).
- 395    12.    Williams, T.A. et al. Visinin-like 1 is upregulated in aldosterone-producing adenomas with  
396       *KCNJ5* mutations and protects from calcium-induced apoptosis. *Hypertension* **59**, 833-839  
397       (2012).
- 398    13.    Akerstrom, T. et al. Activating mutations in *CTNNB1* in aldosterone producing adenomas. *Sci.*  
399       *Rep.* **6**, 19546 (2016).
- 400    14.    Tadjine, M., Lampron, A., Ouadi, L. & Bourdeau, I. Frequent mutations of beta-catenin gene  
401       in sporadic secreting adrenocortical adenomas. *Clin. Endocrinol. (Oxf)* **68**, 264-270 (2008).
- 402    15.    Omata, K. et al. Cellular and genetic causes of idiopathic hyperaldosteronism. *Hypertension*  
403       **72**, 874-880 (2018).
- 404    16.    Teo, A. E. et al. Pregnancy, primary aldosteronism, and adrenal *CTNNB1* mutations. *N. Engl.*  
405       *J. Med.* **373**, 1429-1436 (2015).
- 406    17.    Kalinec, G., Nazarali, A. J., Hermouet, S., Xu, N. & Gutkind, J. S. Mutated alpha subunit of the  
407       Gq protein induces malignant transformation in NIH 3T3 cells. *Mol. Cell. Biol.* **12**, 4687-4693  
408       (1992).
- 409    18.    Gutowski, S. et al. Antibodies to the alpha q subfamily of guanine nucleotide-binding  
410       regulatory protein alpha subunits attenuate activation of phosphatidylinositol 4,5-  
411       bispophosphate hydrolysis by hormones. *J. Biol. Chem.* **266**, 20519-20524 (1991).
- 412    19.    Backman, S. et al. RNA sequencing provides novel insights into the transcriptome of  
413       aldosterone producing adenomas. *Sci. Rep.* **9**, 6269 (2019).
- 414    20.    Wiese, M. et al. The beta-catenin/CBP-antagonist ICG-001 inhibits pediatric glioma  
415       tumorigenicity in a Wnt-independent manner. *Oncotarget* **8**, 27300-27313 (2017).
- 416    21.    Zhou, L. et al. Multiple genes of the renin-angiotensin system are novel targets of Wnt/beta-  
417       catenin signaling. *J. Am. Soc. Nephrol.* **26**, 107-120 (2015).
- 418    22.    Doghman, M., Cazareth, J. & Lalli, E. The T cell factor/beta-catenin antagonist PKF115-584  
419       inhibits proliferation of adrenocortical carcinoma cells. *J. Clin. Endocrinol. Metab.* **93**, 3222-  
420       3225 (2008).

23. Zhou, T. et al. CTNNB1 knockdown inhibits cell proliferation and aldosterone secretion through inhibiting Wnt/beta-catenin signaling in H295R cells. *Technol. Cancer Res. Treat.* **19**, 1533033820979685 (2020).
24. Jeppesen, J. V. et al. LH-receptor gene expression in human granulosa and cumulus cells from antral and preovulatory follicles. *J. Clin. Endocrinol. Metab.* **97**, E1524-E1531 (2012).
25. Breen, S. M. et al. Ovulation involves the luteinizing hormone-dependent activation of G(q/11) in granulosa cells. *Mol. Endocrinol.* **27**, 1483-1491 (2013).
26. Gazdar, A. F. et al. Establishment and characterization of a human adrenocortical carcinoma cell line that expresses multiple pathways of steroid biosynthesis. *Cancer Res.* **50**, 5488-5496 (1990).
27. Tissier, F. et al. Mutations of beta-catenin in adrenocortical tumors: activation of the Wnt signaling pathway is a frequent event in both benign and malignant adrenocortical tumors. *Cancer Res.* **65**, 7622-7627 (2005).
28. Boulkroun, S. et al. Aldosterone-producing adenoma formation in the adrenal cortex involves expression of stem/progenitor cell markers. *Endocrinology* **152**, 4753-4763 (2011).
29. Shaikh, L. H. et al. LGR5 activates noncanonical Wnt signaling and inhibits aldosterone production in the human adrenal. *J. Clin. Endocrinol. Metab.* **100**, E836-E844 (2015).
30. Zhou, J. et al. Transcriptome pathway analysis of pathological and physiological aldosterone-producing human tissues. *Hypertension* **68**, 1424-1431 (2016).
31. Taylor, M. J. et al. Chemogenetic activation of adrenocortical Gq signaling causes hyperaldosteronism and disrupts functional zonation. *J. Clin. Invest.* **130**, 83-93 (2020).
32. Leng, S. et al. beta-Catenin and FGFR2 regulate postnatal rosette-based adrenocortical morphogenesis. *Nat. Commun.* **11**, 1680 (2020).
33. Schwindinger, W. F., Francomano, C. A. & Levine, M. A. Identification of a mutation in the gene encoding the alpha subunit of the stimulatory G protein of adenylyl cyclase in McCune-Albright syndrome. *Proc. Natl. Acad. Sci. USA* **89**, 5152-5156 (1992).
34. Weinstein, L. S. et al. Activating mutations of the stimulatory G protein in the McCune-Albright syndrome. *N. Engl. J. Med.* **325**, 1688-1695 (1991).
35. Idowu, B. D. et al. A sensitive mutation-specific screening technique for *GNAS1* mutations in cases of fibrous dysplasia: the first report of a codon 227 mutation in bone. *Histopathology* **50**, 691-704 (2007).
36. Vasilev, V. et al. McCune-Albright syndrome: a detailed pathological and genetic analysis of disease effects in an adult patient. *J. Clin. Endocrinol. Metab.* **99**, E2029-E2038 (2014).
37. Rey, R. A. et al. Unexpected mosaicism of R201H-*GNAS1* mutant-bearing cells in the testes underlie macro-orchidism without sexual precocity in McCune-Albright syndrome. *Hum. Mol. Genet.* **15**, 3538-3543 (2006).
38. Wu, D. Q., Lee, C. H., Rhee, S. G. & Simon, M. I. Activation of phospholipase C by the alpha subunits of the Gq and G11 proteins in transfected Cos-7 cells. *J. Biol. Chem.* **267**, 1811-1817 (1992).
39. Ayturk, U. M. et al. Somatic activating mutations in *GNAQ* and *GNA11* are associated with congenital hemangioma. *Am. J. Hum. Genet.* **98**, 789-795 (2016).
40. Van Raamsdonk, C. D. et al. Mutations in *GNA11* in uveal melanoma. *N. Engl. J. Med.* **363**, 2191-2199 (2010).
41. Shirley, M. D. et al. Sturge-Weber syndrome and port-wine stains caused by somatic mutation in *GNAQ*. *N. Engl. J. Med.* **368**, 1971-1979 (2013).
42. Thomas, A. C. et al. Mosaic activating mutations in *GNA11* and *GNAQ* are associated with phakomatosis pigmentovascularis and extensive dermal melanocytosis. *J. Invest. Dermatol.* **136**, 770-778 (2016).
43. Simon, D. P. & Hammer, G. D. Adrenocortical stem and progenitor cells: implications for adrenocortical carcinoma. *Mol. Cell. Endocrinol.* **351**, 2-11 (2012).

- 471 44. Berthon, A. et al. WNT/beta-catenin signalling is activated in aldosterone-producing  
472 adenomas and controls aldosterone production. *Hum. Mol. Genet.* **23**, 889-905 (2014).
- 473 45. Lerario, A. M., Moraitis, A. & Hammer, G. D. Genetics and epigenetics of adrenocortical  
474 tumors. *Mol. Cell. Endocrinol.* **386**, 67-84 (2014).
- 475 46. Wang, J. J., Peng, K. Y., Wu, V. C., Tseng, F. Y. & Wu, K. D. *CTNNB1* mutation in aldosterone  
476 producing adenoma. *Endocrinol. Metab. (Seoul)* **32**, 332-338 (2017).
- 477 47. Assie, G. et al. Integrated genomic characterization of adrenocortical carcinoma. *Nat. Genet.*  
478 **46**, 607-612 (2014).
- 479 48. Jakobsen, J. N., Santoni-Rugiu, E., Grauslund, M., Melchior, L. & Sorensen, J. B. Concomitant  
480 driver mutations in advanced *EGFR*-mutated non-small-cell lung cancer and their impact on  
481 erlotinib treatment. *Oncotarget* **9**, 26195-26208 (2018).
- 482 49. Gainor, J. F. et al. *ALK* rearrangements are mutually exclusive with mutations in *EGFR* or  
483 *KRAS*: an analysis of 1,683 patients with non-small cell lung cancer. *Clin. Cancer Res.* **19**,  
484 4273-4281 (2013).
- 485 50. Nanba, K. et al. Genetic characteristics of aldosterone-producing adenomas in Blacks.  
486 *Hypertension* **73**, 885-892 (2019).
- 487 51. Pignatti, E. et al. Beta-catenin causes adrenal hyperplasia by blocking zonal  
488 transdifferentiation. *Cell Rep.* **31**, 107524 (2020).
- 489 52. Vouillarmet, J. et al. Aldosterone-producing adenoma with a somatic *KCNJ5* mutation  
490 revealing APC-dependent familial adenomatous polyposis. *J. Clin. Endocrinol. Metab.* **101**,  
491 3874-3878 (2016).
- 492 53. Polak, P. et al. Cell-of-origin chromatin organization shapes the mutational landscape of  
493 cancer. *Nature* **518**, 360-364 (2015).
- 494 54. Yeh, I. et al. Combined activation of MAP kinase pathway and beta-catenin signaling cause  
495 deep penetrating nevi. *Nat. Commun.* **8**, 644 (2017).
- 496 55. Piaggio, F. et al. Secondary somatic mutations in G-protein-related pathways and mutation  
497 signatures in uveal melanoma. *Cancers (Basel)* **11**, 1688 (2019).
- 498 56. Chen, X. et al. The melanoma-linked "redhead" MC1R influences dopaminergic neuron  
499 survival. *Ann. Neurol.* **81**, 395-406 (2017).
- 500 57. Cavlan, D., Storr, H. L., Berney, D., Evagora, C. & King, P. J. Adrenal pigmentation in PPAD is  
501 a result of melanin deposition and associated with upregulation of the melanocortin 1  
502 receptor. *Endocrine Abstracts* **38**, 154 (2015).
- 503 58. Binder, J. X. et al. COMPARTMENTS: unification and visualization of protein subcellular  
504 localization evidence. *Database (Oxford)* **2014**, bau012 (2014).
- 505 59. de Lau, W. et al. *Lgr5* homologues associate with Wnt receptors and mediate R-spondin  
506 signalling. *Nature* **476**, 293-297 (2011).
- 507 60. Vidal, V. et al. The adrenal capsule is a signaling center controlling cell renewal and zonation  
508 through *Rspo3*. *Genes Dev.* **30**, 1389-1394 (2016).
- 509 61. Yi, H., Wang, Y., Kavallaris, M. & Wang, J. Y. *Lgr4*-mediated potentiation of Wnt/ $\beta$ -catenin  
510 signaling promotes MLL leukemogenesis via an *Rspo3*/Wnt3a-Gnaq pathway in leukemic  
511 stem cells. *Blood* **122**, 887 (2013).
- 512 62. Carter, J. M. et al. *CTNNB1* mutations and estrogen receptor expression in neuromuscular  
513 choristoma and its associated fibromatosis. *Am. J. Surg. Pathol.* **40**, 1368-1374 (2016).
- 514 63. Crago, A. M. et al. Near universal detection of alterations in *CTNNB1* and Wnt pathway  
515 regulators in desmoid-type fibromatosis by whole-exome sequencing and genomic analysis.  
516 *Genes Chromosomes Cancer* **54**, 606-615 (2015).
- 517 64. Maria, A. G. et al. Mosaicism for *KCNJ5* causing early-onset primary aldosteronism due to  
518 bilateral adrenocortical hyperplasia. *Am. J. Hypertens.* **33**, 124-130 (2020).
- 519 65. Zhang, E. D. et al. Mutation spectrum in *GNAQ* and *GNA11* in Chinese uveal melanoma.  
520 *Precis. Clin. Med.* **2**, 213-220 (2019).

521 66. Gerstenblith, M. R., Goldstein, A. M., Fargnoli, M. C., Peris, K. & Landi, M. T. Comprehensive  
522 evaluation of allele frequency differences of *MC1R* variants across populations. *Hum. Mutat.*  
523 **28**, 495-505 (2007).

524 67. Eguchi, K. et al. An adverse pregnancy-associated outcome due to overlooked primary  
525 aldosteronism. *Intern. Med.* **53**, 2499-2504 (2014).

526 68. Saner-Amigh, K. et al. Elevated expression of luteinizing hormone receptor in aldosterone-  
527 producing adenomas. *J. Clin. Endocrinol. Metab.* **91**, 1136-1142 (2006).

528 69. Gagnon, N. et al. Genetic characterization of GnRH/LH-responsive primary aldosteronism. *J.*  
529 *Clin. Endocrinol. Metab.* **103**, 2926-2935 (2018).

530 70. Albiger, N. M. et al. A case of primary aldosteronism in pregnancy: do LH and GNRH  
531 receptors have a potential role in regulating aldosterone secretion? *Eur. J. Endocrinol.* **164**,  
532 405-412 (2011).

533 71. Berthon, A., Drelon, C. & Val, P. Pregnancy, primary aldosteronism, and somatic *CTNNB1*  
534 mutations. *N. Engl. J. Med.* **374**, 1493-1494 (2016).

535 72. Murtha, T. D., Carling, T. & Scholl, U. I. Pregnancy, primary aldosteronism, and somatic  
536 *CTNNB1* mutations. *N. Engl. J. Med.* **374**, 1492-1493 (2016).  
537  
538

**Acknowledgements**

The *CTNNB1* plasmid was a kind gift of Mariann Bienz, Medical Research Council Laboratory of Molecular Biology, Cambridge. The project was funded in part by the British Heart Foundation through a Clinical Research Training Fellowship FS/19/50/34566 and PhD Studentship FS/14/75/31134, by the National Institute of Health Research (NIHR) through Senior Investigator award NF-SI-0512-10052, all to M.J.B., and by NIHR Efficacy and Mechanisms Evaluation Project 14/145/09 and Barts and the London Charity project MGU0360, to W.M.D. and M.J.B. The project was further funded through institutional support from INSERM, the Agence Nationale de la Recherche (ANR-15-CE14-0017-03), and the Fondation pour la Recherche Médicale (EQU201903007864) to M.-C.Z. E.A.B.A. is a Royal Society-Newton Advanced Research Fellow (NA170257/FF-2018-033). R.V.T. is supported by a Wellcome Trust Investigator Award (grant number 106995/Z/15/Z) and the National Institute for Health Research (NIHR) Oxford Biomedical Research Centre Programme. C.P.C. is supported the NIHR Biomedical Research Centre at Barts and The London School of Medicine and Dentistry. The research of J.L.K., Z.T., and R.F. was supported by the National Medical Research Council and Biomedical Research Council of Singapore. Research in London and Cambridge, UK, was further supported by the NIHR Barts Cardiovascular Biomedical Research Centre (BRC), and Cambridge BRC-funded Tissue Bank. The research utilised Queen Mary University of London's Apocrita HPC facility, supported by QMUL Research-IT (<http://doi.org/10.5281/zenodo.438045>). Assistance of the Endocrine Unit Laboratory of the National University of Malaysia (UKM) Medical Centre, and from Long Kha Chin and Siti Khadijah, UKM, is acknowledged.

**Author Contributions**

C.P.C., E.A.B.A. and M.J.B. discovered the mutations in *GNA11* and *GNAQ*, replicated by J.Z. and F.F.-R. J.Z., E.A.B.A., C.P.C., F.F.-R., S. Boulkroun, H.L.S., M.-C.Z., and M.J.B. conceived and designed the subsequent experiments/analyses. C.J., A.T., H.L.S., E.C., G.A., X.W., E.G., L.A., S. Backman, P.H., P.B., T.A., R.S., D.B., J.P.K., W.M.D., L.P. and F.K.F. contributed to cohort ascertainment, phenotypic characterization and recruitment. S. Backman, C.P.C., S.P., Z.T., L.M., T.A., and S.G. contributed to whole-exome/RNA sequencing production, validation, analysis and re-analysis. J.Z., F.F.-R., S. Boulkroun, X.W., A.E.D.T., E.A.B.A., E.C., S.G., G.A., and T.A. performed targeted sequencing and RT-PCR analyses. J.Z. performed the laser capture microdissection (LCM) and genotyping of adrenal zones and biopsy punches. S.J., S. Boulkroun, A.M. and J.Z. performed and F.F.-R. and E.A.B.A. analyzed the immunohistochemistry (IHC) staining. C.E.G S. developed antisera for use in IHC. J.Z., S.G., A.G., K.E.L., and R.V.T. contributed to the plasmid construction for *GNA11* and *GNAQ*. J.Z., E.A.B.A., and G.A. performed the functional experiments on transfected H295R and primary human adrenal cells. J.Z. and S.O. undertook confocal analyses. J.Z., E.A.B.A., F.F.-R., C.A.M., R.F., E.W., D.K., J.L.K., Z.T. and C.P.C. performed the ddPCR, WES and NGS for genotyping of adjacent adrenal regions. C.P.C., J.Z., E.A.B.A., and M.J.B. contributed to statistical analyses. E.A.B.A. and M.J.B. drafted the manuscript, for which J.Z., E.A.B.A., C.P.C., F.F.-R., S. Boulkroun, T.A., A.M., and M.J.B. contributed figures. C.P.C., F.F.-R., S. Boulkroun, M.G., V.K. and M.-C.Z. critically reviewed the text. All authors read and approved the manuscript.

## **Competing Interests Statement**

The authors declare no competing interests.

583 **Figure Legends**

584 **Figure 1 | Clinical and cellular schemas showing the critical roles of GNA11/Q, and their p.Gln209**  
585 **residue, in the production of aldosterone. a,** The renin-angiotensin-aldosterone system is  
586 superimposed on an axial PET CT image through the adrenal glands. The image is taken from the  
587 <sup>11</sup>C-metomidate PET CT of one of the women whose unilateral (left) double-mutant aldosterone-  
588 producing adenoma (APA) was diagnosed by the scan. The hormone-enzyme, renin, is secreted from  
589 the kidneys in response to falls in blood pressure or sodium (Na<sup>+</sup>). Its substrate, the protein  
590 angiotensinogen, is cleaved into an inert decapeptide, angiotensin 1 (Ang I), which is converted on  
591 further cleavage by the angiotensin-converting-enzyme (ACE) into the octapeptide, Ang II. This is a  
592 potent vasoconstrictor and principal physiological stimulus of aldosterone production in the zona  
593 glomerulosa cells of the outer adrenal cortex. The cellular actions of Ang II are mediated by coupling  
594 of its receptor (AT1R) to inositol trisphosphate (IP<sub>3</sub>) and intracellular calcium (Ca<sup>2+</sup>) release, through  
595 a trimeric G-protein whose  $\alpha$  subunit is either G $\alpha$ 11 or G $\alpha$ q. **b,** A single cell of a double-mutant APA,  
596 illustrating similar 2D and 3D-structures of GNA11/Q and GNAS, proximity of the Q209 (GNA11/Q) or  
597 Q227 (GNAS) residue to GDP, and synergism between somatic mutations of *GNA11/Q* and *CTNNB1*,  
598 upregulating luteinizing hormone and human choriogonadotrophin receptor (LHCGR) expression and  
599 production of aldosterone. The Q209 residue of G $\alpha$ 11 or G $\alpha$ q (encoded by GNA11 or GNAQ) and  
600 analogous residue of other G-proteins is essential for GTPase activity<sup>17</sup>. 3D-structures for GNAQ and  
601 GNAS show the p.Gln residue in purple. Somatic or mosaic mutation of p.Gln inhibits GTPase activity  
602 and constitutively activates downstream signalling. We find that p.Gln mutation of GNA11/Q  
603 stimulates aldosterone production, and, in the adrenal, always co-exists with somatic mutation in  
604 exon 3 of *CTNNB1*. This prevents inactivation by phosphorylation (e.g. of p.Ser33, in purple, in the  
605 partial 3D sequence). Double-mutation of GNA11/Q and CTNNB1 induces high expression of multiple  
606 genes, including LHCGR, the G $\alpha$ s/cyclic AMP coupled receptor of luteinizing and pregnancy  
607 hormones. The 3D structures of CTNNB1, GNAS, GNAQ, AT1-receptor, renin, ACE were downloaded  
608 from models 6M93, 3C14, 4QJ3, 6YV1, 2V0Z, 1O8A, respectively, at [www.rcsb.org/](http://www.rcsb.org/).

609

**Figure 2 | Mutations of *GNA11*/Q Q209 increase aldosterone production in human adrenocortical cells.** **a**, Transfection of mutations of *GNA11* Q209 (Q209L, Q209P, and Q209H) into immortalized adrenocortical H295R cells stimulated aldosterone secretion ( $n = 40$  wells examined over 5 independent experiments,  $P = 1 \times 10^{-15}$  by one-way Kruskal-Wallis test,  $\chi^2(4) = 105.78$ ). **b**, *CYP11B2* mRNA expression was increased in H295R cells transfected with *GNA11* mutations ( $n = 12-31$  biologically independent samples,  $P = 9 \times 10^{-9}$  by one-way Kruskal-Wallis test,  $\chi^2(4) = 43.34$ ). **c**, Effect of *GNA11* mutations on aldosterone secretion in H295R cells co-transfected with either scrambled siRNA (SiScrambled) or siRNA targeting *CTNNB1* (SiCTNNB1) ( $n = 12-20$  biologically independent samples). **d**, Effect of *GNA11* mutations on aldosterone secretion in H295R cells in the presence of the selective  $\beta$ -catenin inhibitor ICG-001 ( $3 \mu\text{M}$ ) or vehicle control ( $n = 10$  wells examined over 3 independent experiments). **e**, Cells from APA 351T, wild-type for *CTNNB1* and *GNA11*/Q (genotype presented in **Supplementary Table 2**), were transfected with either wild-type *GNA11* (WT) or *GNA11* Q209H/L only (Q209H/L) or co-transfected with either wild-type *CTNNB1* (WT + WT) or *CTNNB1*  $\Delta 45$  ( $\Delta 45$ ). Double mutations increased aldosterone secretion compared to single mutations ( $n = 3$  independent transfections,  $P = 0.0003$  by one-way ANOVA). **f**, Effect of *GNA11* Q209H mutation on aldosterone secretion in H295R cells ( $n = 10$  wells examined over 3 independent experiments). For box and whiskers plots (**a**, **b**, and **f**), the central line, box and whiskers indicate the median, interquartile range (IQR) and the 10<sup>th</sup>-90<sup>th</sup> percentile, respectively. For bar charts (**c** and **d**) and scatterplots (**e**), data are presented as mean values  $\pm$  s.e.m. Results for **a**, **b**, **d** and **f** are expressed as fold-change from wild-type untreated transfected cells. Results for **c** and **e** are expressed as pM of aldosterone per  $\mu\text{g}$  of protein. The exact sample numbers ( $n$ ) are as indicated below the x-axis.  $P$ -values of Dunn's multiple comparisons test are as indicated in **a** and **b**, whereas the  $P$ -values indicated in graph in **e** are of Bonferroni's multiple comparisons test.  $P$ -values indicated in **c**, **d**, and **f** are according to two-tailed Student's  $t$ -test. ns, not significant. The data used to generate these plots are provided as a Source Data file.



**Figure 3 | High LHCGR expression in *GNA11/Q* and *CTNNB1* double-mutant adrenal cells.** **a**, *LHCGR* mRNA in 10 double-mutant *CTNNB1*-mutated APAs in the discovery UK/Irish cohort was increased compared to 24 *CTNNB1*-negative APAs and 34 control adjacent adrenals ( $P = 0.0001$  by one-way Kruskal-Wallis test,  $\chi^2(2) = 18.02$ ). **b**, *LHCGR* mRNA in five double-mutant APAs in the replication French cohort was increased compared to seven APAs with solitary *CTNNB1* mutations, nine *CTNNB1* negative APAs, and six control normal adrenals ( $P = 0.003$  by one-way Kruskal-Wallis test,  $\chi^2(3) = 13.70$ ). **c**, *LHCGR* mRNA in one double-mutant APA in the replication Swedish cohort compared to two APAs with only *CTNNB1* mutations, 20 *CTNNB1*-negative APAs, and three cortisol-producing adenomas (CPA) ( $P = 0.08$  by one-way Kruskal-Wallis test,  $\chi^2(3) = 6.87$ ). **d**, LHCGR protein is highly expressed in double-mutant APAs that presented at times of high LH/HCG (e.g. patient 6 during menopause and patient 7 during pregnancy) compared to single *CTNNB1*-mutant APAs (e.g. patient F11). Scale bars, 2 mm. **e**, mRNA of *GNA11* (green symbols,  $n = 6$ ), *CTNNB1* (magenta symbols,  $n = 6$ ), and *LHCGR* in APA 392T cells transfected with vector control ( $n = 11$ ),  $\Delta 45$  *CTNNB1* untagged plasmid ( $n = 11$ ), Q209P *GNA11* GFP tagged plasmid ( $n = 12$ ), or co-transfected with both  $\Delta 45$  *CTNNB1* and Q209P *GNA11* plasmids ( $n = 10$ ). *LHCGR* mRNA was increased in double mutant cells ( $P = 0.02$  by one-way Kruskal-Wallis test,  $\chi^2(3) = 9.78$ ). The central line, box and whiskers indicate the median, IQR and the 10<sup>th</sup>-90<sup>th</sup> percentile, respectively. Error bars presents geometric mean  $\pm$  s.d. **f**, Immunofluorescence of GNA11 (green), CTNNB1 (magenta), and LHCGR (red), of cells transfected as in **e**. Scale bars, 50  $\mu$ m. **g**, Corrected Total Cell Fluorescence (CTCF) of LHCGR in cells transfected as in **e** and **f**. Double-mutant cells had higher CTCF compared to vector control ( $P = 0.00005$  by one-way ANOVA). Exact  $n$  numbers indicated below the x-axis. Data presented as mean values  $\pm$  s.e.m.  $P$ -values of Dunn's multiple comparisons test indicated in **a**, **b**, and **e** ( $*P = 0.02$  comparing vector and double-mutant cells) and Holm-Sidak's multiple comparison test in **g**.  $n$ , represents biologically independent samples. Squares, males. Circles, females. Open symbols, fresh-frozen/RNALater–preserved tissues. Close symbols, FFPE tissues. Red symbols, double mutants. Blue symbols, *KCNJ5* mutants. Black symbols, *KCNJ5* wild-type. The data used to generate these plots are provided as a Source Data file.

**Figure 4 | Gene expression profiles in *GNA11/Q* and *CTNNB1* double-mutant adrenal cells.** **a**, Heat map representation of 362 differentially expressed genes (DEG) with large variance ( $\log_2$  difference > 4) among aldosterone-producing adenomas (APA) in at least one of three transcriptome studies (2012 microarray including patient 6<sup>5</sup>, 2015 microarray including patient 4<sup>16</sup>, Swedish RNA-seq<sup>19</sup>). Each column represents the expression profile of the APA ( $n = 38$ ). Both genes and individual APA are hierarchically clustered. The unsupervised cluster analysis of samples, indicated by the bracketing above the heat map, separated the expression profiles of *GNA11/Q* and *CTNNB1* double-mutant APAs (boxed red). Yellow and blue colors indicate high and low expression levels, respectively, relative to the mean (as indicated by the color scale bar). **b**, Zoomed image of the heat map in **a** of six interesting DEG (yellow arrow) that separated double-mutant (DM) APAs from single-mutant APAs (SM) and other APA genotypes. *LHCGR* (red arrow) and *CYP11B1* (black arrow) also clustered the double-mutant APAs together. **c**, The DEG highlighted in **b** were investigated in double-mutant APAs from the UK/Irish cohort compared to *CTNNB1*-negative APAs. All, except for *C9ORF84* (which had a trend), had significantly higher mRNA expression in double mutant APAs (the *P*-values indicated are according to Kolmogorov–Smirnov statistical test). **d–f**, The DEG *TMEM132E* mRNA expression was significantly higher in double mutant APAs from the UK/Irish cohort compared to *CTNNB1*-negative APAs (**d**;  $P = 0.001$  by Kolmogorov–Smirnov test), in double-mutant APAs from the French cohort compared to *CTNNB1* single-mutant APAs (**e**;  $P = 0.0002$  by one-way Kruskal–Wallis test,  $\chi^2(2) = 13.01$ ; *P*-values of Dunn’s multiple comparisons test are as indicated), and in *GNA11* Q209L transfected H295R cells compared to *GNA11* wild-type transfected cells (**f**;  $P = 0.001$  by two-tailed Student’s *t*-test). The central line, box and whiskers indicate the median, IQR and the 10th–90th percentile, respectively. *GNA11* mRNA expression in *GNA11* Q209L and wild-type transfected cells were not significantly different. The exact sample number ( $n$ ), as indicated below the x-axis, represents biologically independent samples. Squares, males. Circles, females. Red symbols, double mutants. Blue symbols, *KCNJ5* mutants. Black symbols, *KCNJ5* wild-type.

**Figure 5 | Aldosterone synthase (CYP11B2) and 11 $\beta$ -hydroxylase (CYP11B1) expression in *GNA11/Q* and *CTNNB1* double-mutant APAs. a,** qPCR analysis of *CYP11B1* and *CYP11B2* mRNA expression found double-mutant APAs to have a lower *CYP11B1:CYP11B2* mRNA expression ratio compared to *CTNNB1* single-mutant APAs or APAs wild-type for *CTNNB1* and *GNA11/Q* (*CTNNB1*-neg APA) ( $P = 0.00004$  by one-way Kruskal-Wallis test,  $\chi^2(2) = 20.23$ ;  $P$ -values of Dunn's multiple comparisons test are as indicated). Results expressed as fold-change from *CTNNB1* wild-type APAs (*CTNNB1*-negative APA). Error bars presents mean  $\pm$  s.e.m. The exact sample number ( $n$ ), as indicated below the x-axis, represents biologically independent samples. Squares, males. Circles, females. Red symbols, double mutants. Blue symbols, *KCNJ5* mutants. Black symbols, *KCNJ5* wild-type. **b,** Immunohistochemistry of CYP11B2 and CYP11B1 in the UK/Irish cohort using the primary antibody anti-CYP11B2 #ab168388 (1:200; Abcam, UK) and anti-CYP11B1 #MABS502, clone 80-7 (1:100; Sigma-Aldrich, USA). The histotype of high CYP11B2 protein expression and low CYP11B1 expression was apparent correlating with the low *CYP11B1:CYP11B2* mRNA expression seen in **a**. Scale bars, 2.5 mm.

**Figure 6 | *GNA11* somatic mutations were found in the adjacent adrenals to double-mutant APAs.**

**a-c, Patient 7. d-f, Patient 1. a,** Genomic DNA from six different regions (R1-R6) in the fresh frozen adrenal sample and the associated RNA from regions 1-3 (R1-R3) were genotyped for *CTNNB1* and *GNA11* mutations. **b,** qPCR of samples in **a** showed 135-151 fold lower mRNA expression level of *CYP11B2* and 16,102-23,987 fold lower mRNA expression level of *LHCGR* in R1 cDNA compared to R2 and R3, respectively. Differentially expressed genes (DEG) highly expressed in double-mutant APAs but lowly expressed in R1 cDNA are presented in **Supplementary Figure 6a. c,** Sanger sequencing of samples in **a** detected solitary *GNA11* Q209H mutation in R1 cDNA and double *CTNNB1* S45F and *GNA11* Q209H mutations in R2 and R3 cDNA. Interestingly, genotyping of R1 genomic DNA (from the exact same sample as R1 cDNA) detected a homozygous *GNA11* Q209H mutation (**Supplementary Fig. 6a**). **d,** Patient 1 was found to have hyperplastic zona glomerulosa (ZG) in adrenal adjacent to double-mutant APA. ZG hyperplasia was demarcated by lack of subcapsular CYP11B1 (visualized using a custom antibody). The hyperplastic ZG was CYP11B2 negative (visualized using a custom antibody) while LHCGR positive (visualized using the antibody NLS1436; 1:200; Novus Biologicals, UK). This phenotype is consistently present in the UK/Irish discovery cohort (**Supplementary Fig. 5c**). **e,** Genomic DNA from the hyperplastic ZG of nine distinct regions of patient 1's adjacent adrenal were collected systematically using segmental laser capture microdissection (LCM) of formalin-fixed paraffin embedded adrenal sections stained with cresyl violet. **f,** Solitary heterozygous and solitary homozygous *GNA11* Q209P somatic mutations were detected in LCM ZG gDNA collected in **e** from regions 1 (ZG1 genomic DNA) and 6 (ZG6 genomic DNA), respectively. ZG samples from other regions were wild-type for both *CTNNB1* and *GNA11* along with the other adrenal zones (**Supplementary Fig. 6b**).

724 **Table 1 | Clinical, biochemical, and *GNA11*/*Q* genotype findings in the discovery cohort of 10 UK/Irish PA patients with *CTNNB1*-mutant APAs**

725 Somatic mutations of *CTNNB1* and *GNA11* in the UK/Irish discovery cohort were detected in patients 1, 2, and 3 by WES of APAs from 41 PA patients.  
726 Patients 4-6 are the three previously reported women<sup>16</sup>, with patient 4’s somatic mutation of *CTNNB1* detected in our first WES<sup>4</sup>.

727

Patient ID	Sex	Age at surgery	Onset presentation	Tumor genotype		Measurements pre-adrenalectomy					Measurements post-adrenalectomy				
				CTNNB1	GNA11/Q	SBP	DBP	Plasma renin	Aldosterone	Serum potassium	SBP	DBP	Plasma renin	Aldosterone	Serum potassium
						mmHg	mmHg	mU/liter	pmol/liter	mmol/liter	mmHg	mmHg	mU/liter	pmol/liter	mmol/liter
GNA11															
1	Male	12	Puberty	S45F	Q209P	180	120	<2	1,358	2.7	110	75	7	74	4.2
2	Female	35	Pregnancy	S45P	Q209P	155	85	<2	559	2.6	123	76	16	283	4.0
3	Female	20	Pregnancy	T41A	Q209H	215	120	<2	1,330	2.5	121	68	N/A	N/A	N/A
4	Female	34	Pregnancy	S33C	Q209H	190	100	<2	2,885	2.0	111	69	31	250	4.1
5	Female	26	Pregnancy	S45F	Q209H	140	86	<2	2,590	2.0	120	70	N/A	N/A	N/A
6	Female	52	Menopause	G34R	Q209P	190	100	<2	672	3.1	118	79	9.0	158	4.1
7	Female	39	Pregnancy	S45F	Q209H	160	101	<2	2,382	2.5	120	83	16.1	124	4.7
8	Female	41		S45F	Q209P	160	90	<2	480	3.2	101	65	91	236	4.5
GNAQ															
9	Female	23	Pregnancy	G34E	Q209H	167	114	<2	2000	3.3	121	85	N/A	N/A	N/A
10	Female	26	Pregnancy	G34R	Q209L	170	110	<2	603	4.1	123	78	14	408	4.7

728 N/A, not available. SBP, systolic blood pressure. DBP, diastolic blood pressure. Units of measurements pre- and post-adrenalectomy are shown in italics.  
729 Bold denotes the name of the gene (*GNA11*/*GNAQ*) in which the Q209 mutation was found.

730  
731

**Table 2 | Clinical presentation and genotype of *GNA11*/Q/S in the APA of 17 primary aldosteronism patients who had *CTNNB1*-mutant APAs from the replication cohorts**

Replication cohort	Patient ID	Sex	Age PA	Hypertensive at pregnancy (number of pregnancies)	Tumor genotype						
					<i>CTNNB1</i> genotype	<i>GNA11</i> Q209	<i>GNA11</i> R183	<i>GNAQ</i> Q209	<i>GNAQ</i> R183	<i>GNAS</i> Q227	<i>GNAS</i> R201
French cohort	F1	Female	29	Yes (1)	S45F	WT	WT	WT	WT	WT	WT
	F2	Male	40	-	S45P	WT	WT	WT	WT	WT	WT
	F3	Female	35	No (2)	S37C	WT	WT	WT	WT	WT	WT
	F4	Male	33	-	S45A	WT	WT	WT	WT	WT	WT
	F5	Female	43	No (1)	S45F	Q209P	WT	WT	WT	WT	WT
	F6	Female	45	Yes (2)	S45P	WT	WT	WT	WT	WT	WT
	F7	Female	55	N/A	S45P	WT	WT	WT	WT	WT	WT
	F8	Female	55	N/A	S45P	WT	WT	WT	WT	WT	WT
	F9	Female	26	Yes* (1)	S37P	WT	WT	Q209H	WT	WT	WT
	F10	Female	51	Yes (1)	S45P	Q209H	WT	WT	WT	WT	WT
	F11	Male	36	-	S45P	WT	WT	WT	WT	WT	WT
	F12	Female	56	No (10)	D32Y	Q209H	WT	WT	WT	WT	WT
	F13	Female	56	No (0)	S45Y	WT	WT	WT	WT	WT	WT
	F14	Female	17	No <sup>#</sup> (0)	G34V	WT	WT	Q209H	WT	WT	WT
Swedish cohort	S1	Female	55	Yes <sup>†</sup> (2)	S45P	WT	WT	Q209H	WT	WT	WT
	S2	Female	59	N/A	S45P	WT	WT	WT	WT	WT	WT
	S3	Female	26	N/A	S37F	WT	WT	WT	WT	WT	WT

732 PA, primary aldosteronism. N/A, not available. WT, wild-type. \*pre-eclampsia. #hypertensive at puberty. †onset at age 24 years old preceding first  
733 pregnancy.

## Online Methods

**Patient cohorts.** All patients were confirmed to have primary aldosteronism by raised aldosterone/renin ratio, positive confirmatory tests and lateralization studies (CT/PET CT<sup>73</sup>, MRI and AVS) according to the institutional protocols at the various centres and in accordance with the Endocrine Society guidelines<sup>74,75</sup>. All patients gave written informed consent for genetic and clinical investigation according to local ethics committee guideline (Cambridgeshire Research Ethics Committee for Addenbrooke's Hospital, University of Cambridge or the Cambridge East Research Ethics Committee for St Bartholomew's Hospital, Queen Mary University of London for the UK cohort; Assistance Publique-Hôpitaux de Paris Research Ethics Committee for the French cohort; Regional Ethical Review Board in Uppsala for the Swedish cohort).

*UK/Irish cohort.* The seven patients with double-mutations of *CTNNB1* and *GNA11* were among 117 UK/Irish patients who were investigated at St Bartholomew's Hospital, London or Addenbrooke's Hospital, Cambridge, or whose operative specimen was received for investigation, during the period 2004 to 2017.

*French cohort.* Patients with primary aldosteronism were recruited between 1999 and 2016 within the COMETE (COrtico- et MEduillo-surrénale, les Tumeurs Endocrines) network (COMETE-Hôpital Européen Georges Pompidou protocol authorization CPP 2012-A00508-35). 198 patients were screened for *CTNNB1* mutations. For some of the patients included in this study, the genetic screening of mutations in *KCNJ5*, *ATP1A1*, *CACNA1D* and *ATP2B3* was previously described<sup>27,76</sup>.

*Swedish cohort.* 15 tumors were selected from a previously documented international cohort<sup>19,77</sup>. Adrenal specimens were collected from 348 patients from centres in Sweden, Germany, France and Australia.



**Whole exome sequencing (WES).** WES of 40 pairs of APAs and adjacent adrenal from UK patients was conducted in the Barts and London Genome Centre, and the Cardiovascular Research Institute of the University of Singapore, with overlap of eight pairs of samples, and previously genotyped controls ( $n = 3$  in each centre/institute) as validation of sensitivity (not included in analysis). The 41<sup>st</sup> APA was analyzed together with germline DNA from blood processed commercially by GATC Biotech, Germany. MuTect2 analysis was conducted in order to identify adrenocortical genes with somatic mutations, predicted by Sorting Intolerant from Tolerant (SIFT) and Polymorphism Phenotyping (PolyPhen)-2 to be functional. Candidate mutations were confirmed by Sanger sequencing of DNA from fresh samples of the APA, and sought in other previously genotyped APAs that were not included in the WES.

*Quality control of WES samples.* Genomic DNA of samples was quality assessed by gel electrophoresis, Agilent 2200 TapeStation and Genomic DNA screentape (Agilent Technologies, Waldbronn, Germany), or as per GATC Biotech standard protocol. Samples with low degradation and a majority of high molecular weight were taken forward for WES.

*WES of patient 1.* WES using the Illumina HiSeq 2000 Sequencer was conducted on DNA extracted from the APA along with the paired germline DNA extracted from the venous blood (samples processed commercially by GATC Biotech, Germany). WES samples were prepared as an Illumina sequencing library and the sequencing libraries were enriched using the Agilent SureSelectXT Human All Exon V6 Kit. The captured libraries were sequenced and downstream analysis conducted as described below.

*WES of patient 2.* WES using the Illumina NextSeq 500 Sequencer was conducted on genomic DNA extracted from APAs from 21 PA patients along with paired adjacent normal adrenal and APAs from three primary aldosteronism patients with known genotype (as sensitivity controls). 50 ng of each DNA sample was processed using the Nextera Rapid Capture Enrichment kit, with the Coding Exome Oligo (CEX) pool. Tagmented DNA was assessed using the Agilent 2200 TapeStation in conjunction with the HSD1000 screentape. All samples showed expected fragmentation profiles with an average fragment

size of 300 bp. Enriched libraries were validated using the Agilent 2200 TapeStation in conjunction with the D1000 screenTape. Equimolar amounts of each sample library were pooled together for sequencing which was carried out using the Illumina NextSeq®500 high-output kit.

*WES of patient 3.* WES using the Illumina HiSeq 2500 sequencer was conducted on genomic DNA extracted from 27 APAs along with paired adjacent normal adrenal and three APAs with known genotype (as sensitivity controls). 1 µg of genomic DNA was fragmented using sonication (Covaris, S220), optimized to give a distribution of 200-500 bp that was verified using a 2100 Bioanalyzer (Agilent, G2939BA). Library preparation was carried out using Kapa DNA HTP Library Preparation Kit (KAPA Biosystems, 07 138 008 001). Hybridization of adapter ligated DNA was performed at 47 °C, for 64 to 72 h, to a biotin-labelled probe included in the Nimblegen SeqCap EZ Human Exome Kit (Roche, 06465692001). Libraries were sequenced using the Illumina HiSeq 2500 sequencing system and paired-end 101-bp reads were generated for analysis with 100x coverage per sample.

*WES data analysis.* Variant calling was performed using Burrows-Wheeler Aligner (BWA) v. 0.7.12 (for 341T) or v. 0.7.15 to align raw reads in the FASTQ files to human reference genome GRCh37. The alignments were sorted and marked for PCR duplicates using Picard Tools software v.1.119 (for 341T) or v.1.7. This was followed by base quality score recalibration (BQSR) using the genome analysis toolkit (GATK) for tuning the quality scores to reflect higher accuracy of base qualities. For 341T, ContEst from GATK was used to calculate cross-sample contamination between samples, using blood as the “normal” versus each of the APA samples. A panel of normals was created from the blood sample of the boy using dbSNP and COSMIC as reference. In order to enrich the panel of normals, we utilize WES of 11 other blood samples, all pre-processed using the same protocol as described above. Resulting BAMs were analyzed with GATK MuTect v.2 software to identify somatic variants. Normal and tumor pairs were analyzed together when available. For tumor-only samples, the MuTect tumor-only algorithm was used. The contamination estimates derived from ContEst, and the dbSNP, COSMIC, the blood sample and the panel of normals were used as resources in the input parameters to filter variants observed in

the germline samples. SNPs, with a threshold coverage of at least 10 reads on the respective nucleotide, were assessed. Oncotator was used to annotate the variants passing the filters (<http://www.broadinstitute.org/oncotator>).

**Re-analysis of RNA-seq data of Swedish cohort.** RNA sequencing previously described in Backman et al.<sup>19</sup> was used for variant identification and analysed for gene expression differentiation.

*RNA-seq variant detection.* RNA-seq variant detection was performed following the recommendations on the GATK workflow for RNA-seq variant discovery. RNA-seq reads were aligned to the UCSC hg19 reference genome using the STAR 2-pass method for sensitive novel junction discovery. Picard tools software (picard-tools-1.119) was then used to sort and mark PCR duplicates on the alignments. The SplitNCigarReads function from GATK was used to reformat alignments, by splitting reads into exon segments, and to reassign reads with good mapping quality into a GATK format. We performed an indel realignment step followed by the quality score recalibration protocol. Variants were called using the HaplotypeCaller from GATK using the ‘-dontUseSoftClippedBases’ parameter and setting the minimum phred-scaled confidence threshold to 20 (-stand\_call\_conf 20.0). The following hard filters were applied to the called variants: ‘-window 35 -cluster 3 -filterName FS -filter "FS > 30.0" -filter Name QD -filter "QD < 2.0"’. Variant annotation was performed using ANNOVAR.

*Comparison of CTNNB1-only mutants with double-mutants.* Gene expression differentiation of the three samples with the CTNNB1 mutation was performed as follows. RNA-seq fastq files were pseudo-aligned to the human GRCh37 cDNA reference sequences from ENSEMBL using kallisto v0.46.0. Transcript abundance was quantified using the kallisto ‘quant’ function with default settings. Gene expression analysis was performed with DESeq2 (v1.24.0). Genes with less than 10 reads were removed from further analysis. Dispersion estimates and size factors were calculated using all 15 samples, with gender as a covariate in the design matrix. The two single-mutation samples were then compared to the sample with a double-mutation.

832

833 **Sanger sequencing of *CTNNB1* and *GNA11/Q/S*. Laser capture microdissection (LCM) of adrenal zones.**

834 Freshly sectioned 10 µm FFPE adrenal sections of patient 1 were used for LCM. Serial adrenal sections  
835 were fixed and rehydrated in ethanol then stained by cresyl violet (Sigma-Aldrich, USA) for 1 min. The  
836 sections were then dehydrated in ethanol and cleaned in Histo-clear II (AGTC Bioproducts Ltd, UK). After  
837 fixing and staining the adrenal sections, ZG cells were collected by LCM technique using a Zeiss PALM  
838 Microbeam laser microdissection system (Carl Zeiss Microscopy, USA) with PALMRobo v4.3 software  
839 according to the manufacturer's instructions. All the pooled ZG LCM samples collected from the same  
840 area of adrenal sections were then stored at -20 °C until RNA and genomic DNA extraction.

841 *Nucleic acid extraction.* Genomic DNA (gDNA) from fresh frozen/RNALater solution–preserved  
842 tissue samples was extracted using Reliaprep™ gDNA Tissue miniprep system (Promega, USA). gDNA  
843 from FFPE samples collected by LCM were extracted using Arcturus® PicoPure® DNA Extraction Kit  
844 (Applied Biosystems™, USA). gDNA of blood from patient 1 and patient 7 were extracted using  
845 Nucleon™ BACC3 Genomic DNA Extraction Kit (GE Healthcare Life Sciences, UK) according to  
846 manufacturer's recommendation.

847 For the UK/Irish cohort, total DNA-free RNA was isolated from fresh frozen/RNALater solution–  
848 preserved samples using TRIzol (Ambion Life Technologies, Carlsbad CA) and PureLink® RNA Mini Kit  
849 (Invitrogen™, USA) according to manufacturer's recommendation. The PureLink® DNase Set was used in  
850 combination to remove DNA from RNA (Invitrogen, USA) by on-column digestion. If the fresh  
851 frozen/RNALater solution–preserved samples were not available, total RNA and gDNA were extracted  
852 from FFPE tissue samples blocks using AllPrep DNA/RNA FFPE Kit (Qiagen, USA) according to  
853 manufacturer's recommendation (FFPE extracted DNA/RNA is reported when used). This kit is also used  
854 on fresh frozen samples when RNA and gDNA from the same sample were required. Total RNA from  
855 FFPE samples collected by LCM were extracted by Arcturus™ Paradise™ Plus RNA Extraction and  
856 Isolation Kit (Applied Biosystems™, USA) in combination with the PureLink® DNase Set, according to

manufacturer's recommendation. After extraction reverse transcription was performed using the High Capacity RNA-to-cDNA kit (Fisher Scientific, USA) according to manufacturer's instructions. The cDNA was purified by DNAClear™ Purification Kit (Invitrogen™, USA).

For the French cohort, total RNA was extracted using Janke and Kunkel's Ultra-Turrax T25 (IKA technologies, Staufen DE) in Trizol reagent (Ambion Life Technologies, USA) according to the manufacturer's recommendations. After deoxyribonuclease I treatment (Life Technologies, USA), 500 ng of total RNA were retro-transcribed (iScript reverse transcriptase, Bio-Rad, USA).

*PCR and sequencing of CTNNB1 and GNA11/Q/S.* Primers used for *CTNNB1*, *GNA11*, *GNAQ* and *GNAS* amplification in gDNA and cDNA samples are described in **Supplementary Tables 5 and 6** or as previously described<sup>16,76</sup>. For UK/Irish cohort, PCR was performed on 100 ng of DNA in a final volume of 20 µl reaction using AmpliTaq Gold™ Fast PCR Master Mix (Thermo Fisher, USA) according to manufacturer's instructions. Sanger sequencing of PCR products was performed using LIGHTRUN Tube sequencing service from Eurofins (Germany). For the French cohort, PCR was performed on 100 ng of DNA in a final volume of 25 µl containing 400 nM of each primer, 200 µM deoxynucleotide triphosphate and 1.25 U Taq DNA Polymerase (Sigma-Aldrich, USA). Sanger sequencing of PCR products was performed using the Big Dye™ Terminator v3.1 Cycle Sequencing Kit (Applied Biosystems, USA) on an ABI Prism 3700 DNA Analyzer (Applied Biosystems, USA). Sanger Sequencing alignment was performed using GATC Viewer 1.00 or BioEdit version 7.2.5.

**Droplet digital PCR (ddPCR) of GNA11/Q.** Specific droplet digital PCR (ddPCR) assays for *GNA11* (c.627 A>C, c.627 A>T, and c.626A>C) and *GNAQ* (c.627A>C and c.627A>T) mutation detection were designed on the Bio-Rad's Digital Assay Site. Each ddPCR reaction mixture (20 µL) contained 45 ng of DNA template, 1 µL of 20X WT (HEX) and mutant (FAM) assays, 4U of restriction enzyme HindIII (New England Biolabs), and 10 µL of 2X Bio-Rad ddPCR Supermix. The reaction mixture was mixed with 70 µL Bio-Rad droplet generator oil and partitioned into 15,000–20,000 droplets by using the QX-100 droplet

generator (Bio-Rad), and transferred to a 96-well PCR reaction plate. PCR conditions were 10 min at 95 °C, 40 cycles of denaturation for 30 s at 94 °C and extension for 60 s at 57 °C with ramp rate of 2.5 °C/s, followed by 10 min at 98 °C. The plate was then transferred to the QX-100 droplet reader (Bio-Rad). QuantaSoft software version 1.3.2.0 (Bio-Rad) was used to quantify the copies of target DNA. The ratio of positive HEX and positive FAM events was used to identify the presence and the proportion of target mutations.

**NGS targeted sequencing of *CTNNB1* and *GNA11/Q/S*.** *French centre.* Immunohistochemistry-guided next generation sequencing (CYP11B2 IHC-guided NGS) was performed as previously described<sup>8</sup>. Before DNA extraction from FFPE tissue, APA was identified by CYP11B2 IHC and the areas of interest were delimited and isolated for DNA extraction by scraping unstained FFPE sections guided by the CYP11B2 IHC slide using a scalpel under a Wild Heerbrugg or Olympus microscope. DNA was extracted from FFPE sections using the AllPrep DNA/RNA FFPE kit (Qiagen). NGS was performed using an amplicon based NGS kit on an Illumina MiSeq sequencer as previously described<sup>78</sup>.

*British centre.* Assays were designed using Primer3 and 5' tagged with Fluidigm TSP sequences to allow barcoding and adapter addition. Samples were PCR amplified with FastStart High Fidelity (Roche) with cycling conditions 95 °C, 2 min, 35 cycles (95 °C, 30 s; 55 °C, 30 s; 72 °C, 30 s), and 72 °C for 5 min on an MJ tetrad MJ225. PCRs were checked on 2% agarose gel. 1 ml of a 1 in 100 dilution of PCR product was used in a second round of PCRs to add Barcodes and Illumina adapters with cycling conditions 95 °C, 10 min, 15 cycles (95 °C, 30 s; 60 °C, 30 s; 72 °C, 30 s), and 72 °C for 3 min on an MJ tetrad MJ225. Products were quantified by Qubit and loaded onto an Illumina NextSeq 500 to generate in excess of 1,000x 75-bp paired end reads. Reads were aligned to human hg38 using BWA and BAM files visualized in IGV.

**WES for validation.** WES was performed for validation for some samples listed in **Supplementary Table 4**. Using the Illumina Hiseq 4000 sequencer was conducted on genomic DNA. 1 µg of genomic DNA was fragmented using sonication (Covaris, S220), optimized to give a distribution of 200-500 bp that was verified using a 2100 Bioanalyzer (Agilent, G2939BA). Library preparation was carried out using Kapa DNA HTP Library Preparation Kit (KAPA Biosystems, 07 138 008 001). Hybridization of adapter ligated DNA was performed at 47 °C, for 64 to 72 h, to a biotin-labelled probe included in the Nimblegen SeqCap EZ Human Exome Kit (Roche, 06465692001). Libraries were sequenced using the Illumina Hiseq 4000 sequencing system and paired-end 150-bp reads were generated for analysis with 200x coverage per sample. Exome data were analyzed using GATK v3.7 with the human\_g1k\_v37\_decoy as reference genome. Annotation of variants was performed using annovar (version 10-24-2019) and in-house pipelines.

**Functional analyses in human adrenocortical cells.** *Construction of wild-type and mutant vectors.* *GNA11* wild-type and Q209L plasmids was kindly given by Rajesh V. Thakker (University of Oxford), constructed in a pBI-CMV2 vector. *CTNNB1* wild-type and del45 (*CTNNB1* Δ45) plasmids were kindly given by Mariann Bienz (University of Cambridge), constructed in a pcDNA3 vector. *GNA11* Q209H and Q209P were generated using the NEB Q5® Site-Directed Mutagenesis Kit (New England Biolabs, UK) using the following primers in **Supplementary Table 7** according to the manufacturer's recommendation.

*Functional assays in H295R and primary human adrenal cells.* The human adrenocortical carcinoma cell line H295R and primary human adrenal cells were cultured as previously described<sup>16</sup>. H295R cells and primary human adrenal cells were transfected with pBI-CMV2 empty vector, *GNA11* wild-type, *GNA11* Q209H/L/P plasmids, with/or without the co-transfection of *CTNNB1* wild-type, *CTNNB1* Δ45 plasmids by electroporation using the Neon™ Transfection System 10/100 µL Kit (Invitrogen™, USA).

For H295R cells, 48 h after transfection, the culture medium was replaced with serum free medium with or without 10 nM angiotensin II (Ang II) or 3 or 10  $\mu$ M of the CTNNB1 inhibitor ICG-001 (AdooQ BioScience, USA). Supernatant was collected for aldosterone measurement after 24 h and cells were harvested for mRNA expression analysis and protein quantification. For primary adrenal cells, supernatant was collected for aldosterone measurement at 24, 27 (+3), 30 (+6) and 48 (+24) h post-transfection and cells were harvested for mRNA expression analysis and protein quantification at the last time point (48 h post-electroporation). All cells harvested for mRNA expression analysis was kept at -80 °C in Trizol until batch extraction of nucleic acid and protein.

*Aldosterone and cortisol measurement.* Aldosterone secretion of primary human adrenal cells was measured using the Homogeneous Time Resolved Fluorescence (HTRF®) Aldosterone competitive assay (Cisbio, France) according to manufacturer's recommendation. Aldosterone secretion was measured on the IDS-iSYS Automated System (#IS-3300, Immunodiagnostic Systems, Germany) for H295R cells at the National University of Malaysia and by Aldosterone HTRF kit (#64ALDC0A, Cisbio, France) using FLUOstar Omega plate reader (BMG labtech) at Queen Mary University of London for primary adrenal cells. The cortisol levels were measured using ECLIA-Technology (Cobas e411, Roche, Germany) and immunoassay for the in vitro quantitative determination of cortisol (#06687733 190, Roche, Germany). Aldosterone and cortisol results were normalized by protein amount estimated by Pierce BCA Protein Assay Kit (Thermo Fisher Scientific, USA) according to manufacturer's recommendation.

**RT-qPCR analyses.** *RT-qPCR analysis of the UK/Irish Cohort and adrenocortical cells.* mRNA expression of genes of interest was quantified using commercially available TaqMan gene expression probes (Thermo Fisher Scientific, USA) listed in **Supplementary Table 8**. The RT-qPCR was performed using the C1000 Touch Thermal Cycler machine (Bio-Rad, USA) or the 7000 SDS (Applied Biosystems, USA) according to



manufacturer's recommendation. Results were analysed using the  $2^{-\Delta\Delta CT}$  method using the housekeeping 18S rRNA (Thermo Fisher Scientific, USA) for normalization.

*RT-qPCR analysis of APAs from the French cohort.* Primers used for *LHCGR*, *CYP11B1* and *CYP11B2* RT-qPCR are described in **Supplementary Table 9**. RT-qPCR was performed using SsoAdvanced Universal SYBR Green Supermix (Bio-Rad, USA) on a Bio-Rad C1000 touch thermal cycler (CFX96 Real Time System) according to the manufacturer's instructions. CFX Manage TM Software v3.1 (Bio-Rad, USA) was used for qPCR data acquisition. Normalization for RNA quantity and reverse transcriptase efficiency was performed against three reference genes (geometric mean of the expression of Ribosomal 18S RNA, *GAPDH* and *HPRT*; primers are described in **Supplementary Table 9**), in accordance with the MIQE guidelines<sup>79</sup>. Quantification was performed using the standard curve method. Standard curves were generated using serial dilutions from a cDNA pool of all samples. Fold change over control adrenals excised from patients who had undergone enlarged nephrectomies for renal carcinoma (*LHCGR* RT-qPCR) and over non-*CTNNB1* mutated APA (*CYP11B1* and *CYP11B2* RT-qPCR) were then calculated.

**Protein expression analyses. Immunohistochemistry (IHC).** The primary antibodies used for IHC are as follows: anti-LHCGR #NLS1436 (1:200; Novus Biological, USA), anti-CYP11B1 (1:100) and anti-CYP11B2 (1:100) gifted by Celso E. Gomez-Sanchez<sup>78</sup>, two commercial anti-CYP11B2 #ab168388 (1:200; Abcam, UK) and #MABS1251 (1:2,500; Sigma-Aldrich, USA), and one commercial anti-CYP11B1 #MABS502 (1:100; Sigma-Aldrich, USA). The secondary antibodies used in the IHC are as follows: affinity purified goat anti-rabbit antibody for LHCGR antibody #BA-1000 (1:400; Vector laboratories, USA), affinity purified horse anti-mouse antibody for CYP11B2 antibody #BA-2000 (1:400; Vector Laboratories, USA), and affinity purified rabbit anti-rat antibody for CYP11B1 antibody #BA-4001 (1:400; Vector Laboratories, USA).

*Immunofluorescence (IFC).* 48 h after electroporation, transfected H295R and primary human adrenal cells were processed for IFC as previously described<sup>16</sup>. Cells were incubated with anti-LHCGR

#NLS1436 (1:200; Novus Biologicals, UK) and anti-CTNNB1 #610154 (1:100; BD transduction Lab, USA) at room temperature for 1 h and then with goat anti-rabbit IgG (H+L) cross-adsorbed secondary antibody, Alexa Fluor 568 (A-11011, 1:1000; Invitrogen, USA) and goat-anti-mouse IgG (H+L) cross-adsorbed secondary antibody, Alexa Fluor 647 (A-21235, 1:1000; Invitrogen, USA) at room temperature for 1 h. Immunofluorescence was visualized using a Zeiss LSM 710 (for ADR351T and 357T)/880 (for ADR392T) confocal microscopes. A second set of primary antibodies, a combination of anti-LHCGR #NBP2-52504 (1:100; Novus Biologicals, UK) and anti-CTNNB1 #71-2700 (1:100; Thermo Fisher Scientific, USA) was used for validation of first set of primary antibodies used. For the second set of primary antibodies, Alexa Fluor 405 (A-31553, 1:1,000; Invitrogen, USA), Alexa Fluor 647 (A-21235, 1:1,000; Invitrogen, USA) and Alexa Fluor 568 (A-11011, 1:1,000; Invitrogen, USA) were used as the secondary antibodies. Zen Blue 21 Edition software (Zeiss, Germany) was used for confocal microscopy image acquisition. Quantification of immunofluorescence was performed using (Fiji Is Just) ImageJ v1.52e Java 1.8.0\_66 as published online (Fitzpatrick, M. Measuring cell fluorescence using ImageJ. *The Open Lab Book*. <https://theolb.readthedocs.io/en/latest/imaging/measuring-cell-fluorescence-using-imagej.html>). Cells successfully transfected with  $\Delta 45$  CTNNB1 was defined based on having a corrected total cell fluorescence (CTCF) for CTNNB1 >100,000.

**Statistical analysis.** All parametric data are presented as mean  $\pm$  s.e.m. For non-parametric data, results were presented as median  $\pm$  95% confidence interval or as geometric mean  $\pm$  95% confidence interval (for qPCR data only). For parametric data, two-tailed Student's *t*-test and one-way or two-way ANOVA statistical tests were performed depending on the grouping factors. Kolmogorov-Smirnov test (when comparing 2 groups) or Kruskal-Wallis test (when comparing >2 groups) was used for non-parametric data. Tests for normality/lognormality and adjustment for multiple comparisons were performed. All the analysis was performed using GraphPad Prism software (version 7.04 and version 9.0.1) or Microsoft Excel v.2016 (for Student's *t*-test). *P*-values lower than 0.05 were considered statistically significant.

1005

1006 **Data Availability Statement**

1007 Source data for **Figure 2a-f** and **Figure 3a-c,e,g** are provided with the paper. The raw RNA-seq dataset  
1008 analyzed to generate **Figure 4a,b**, **Supplementary Table 3** and **Supplementary Figure 4** is available upon  
1009 requests to the Science for Life Laboratory Data Centre through the DOI link  
1010 <https://doi.org/10.17044/NBIS/G000007>. Regulations by the service provider may make access  
1011 technically restricted to PIs at Swedish organizations. The microarray datasets analyzed to generate  
1012 **Figure 4a,b** are deposited in the Gene Expression Omnibus database (GSE64957) or are available from  
1013 the corresponding author on reasonable request. The whole exome sequencing raw data of the 41 APAs  
1014 and controls investigated for recurrent pathogenic somatic mutation are available from the Sequence  
1015 Read Archive (SRA) under the accession numbers PRJNA732946 and PRJNA729738. All other raw data  
1016 that support the findings of this study are available from the corresponding author upon reasonable  
1017 request.

1018

1019 **Methods-only References**

- 1020 73. Burton, T. J. et al. Evaluation of the sensitivity and specificity of (11)C-metomidate positron  
1021 emission tomography (PET)-CT for lateralizing aldosterone secretion by Conn's adenomas. *J.*  
1022 *Clin. Endocrinol. Metab.* **97**, 100-109 (2012).
- 1023 74. Letavernier, E. et al. Blood pressure outcome of adrenalectomy in patients with primary  
1024 hyperaldosteronism with or without unilateral adenoma. *J. Hypertens.* **26**, 1816-1823 (2008).
- 1025 75. Funder, J. W. et al. Case detection, diagnosis, and treatment of patients with primary  
1026 aldosteronism: an endocrine society clinical practice guideline. *J. Clin. Endocrinol. Metab.* **93**,  
1027 3266-3281 (2008).

1028 76. Fernandes-Rosa, F. L. et al. Genetic spectrum and clinical correlates of somatic mutations in  
1029 aldosterone-producing adenoma. *Hypertension* **54**, 354-361 (2014).

1030 77. Akerstrom, T. et al. Comprehensive re-sequencing of adrenal aldosterone producing lesions  
1031 reveal three somatic mutations near the KCNJ5 potassium channel selectivity filter. *PLoS One* **7**,  
1032 e41926 (2012).

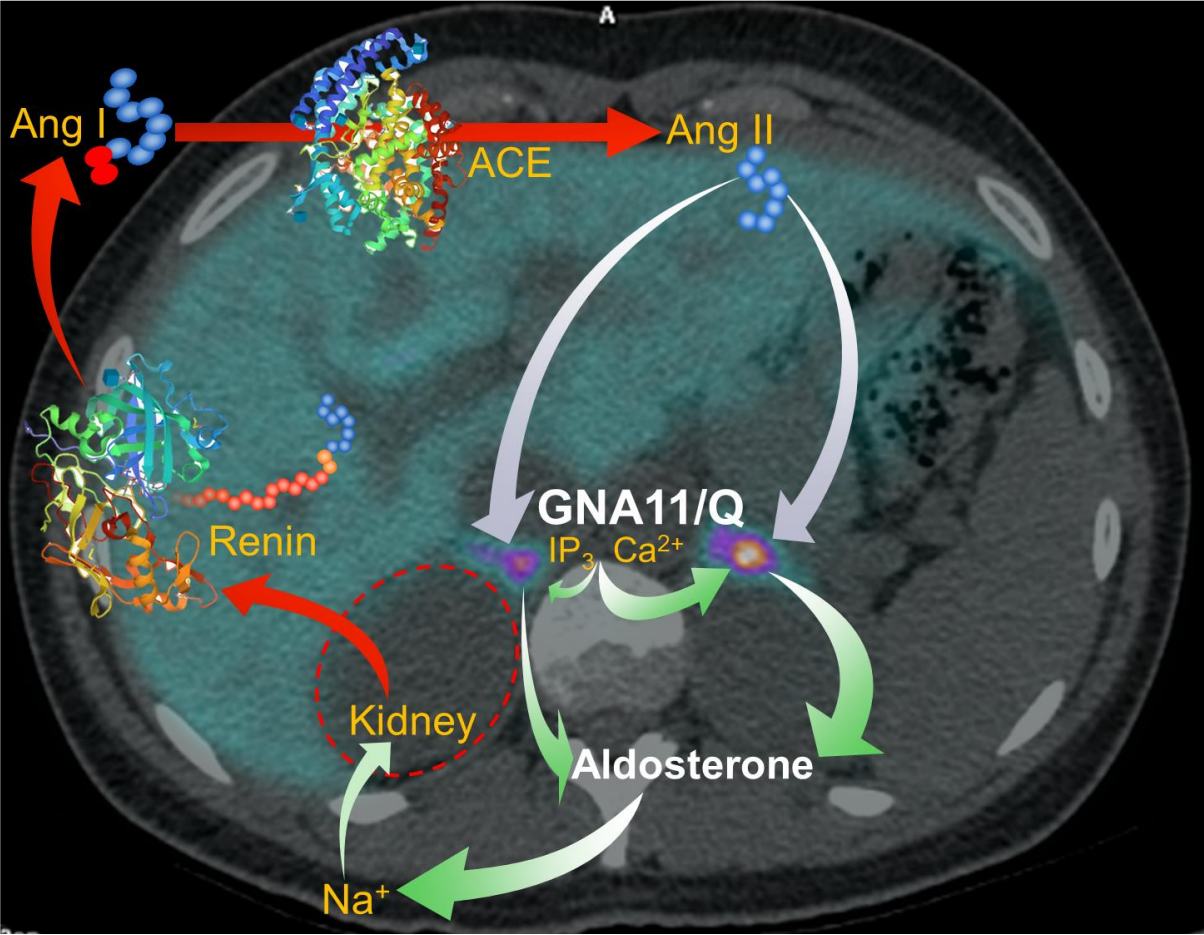
1033 78. Gomez-Sanchez, C. E. et al. Development of monoclonal antibodies against human CYP11B1 and  
1034 CYP11B2. *Mol. Cell. Endocrinol.* **383**, 111-117 (2014).

1035 79. Bustin S. A. Why the need for qPCR publication guidelines? The case for MIQE. *Methods* **50**, 217-  
1036 226 (2010).

1037

Figure 1 (a-b)  
Clinical (a) and cellular (b) schemas showing the critical roles of GNA11/Q, and their p.Gln209 residue, in the production of aldosterone.

a.



b.

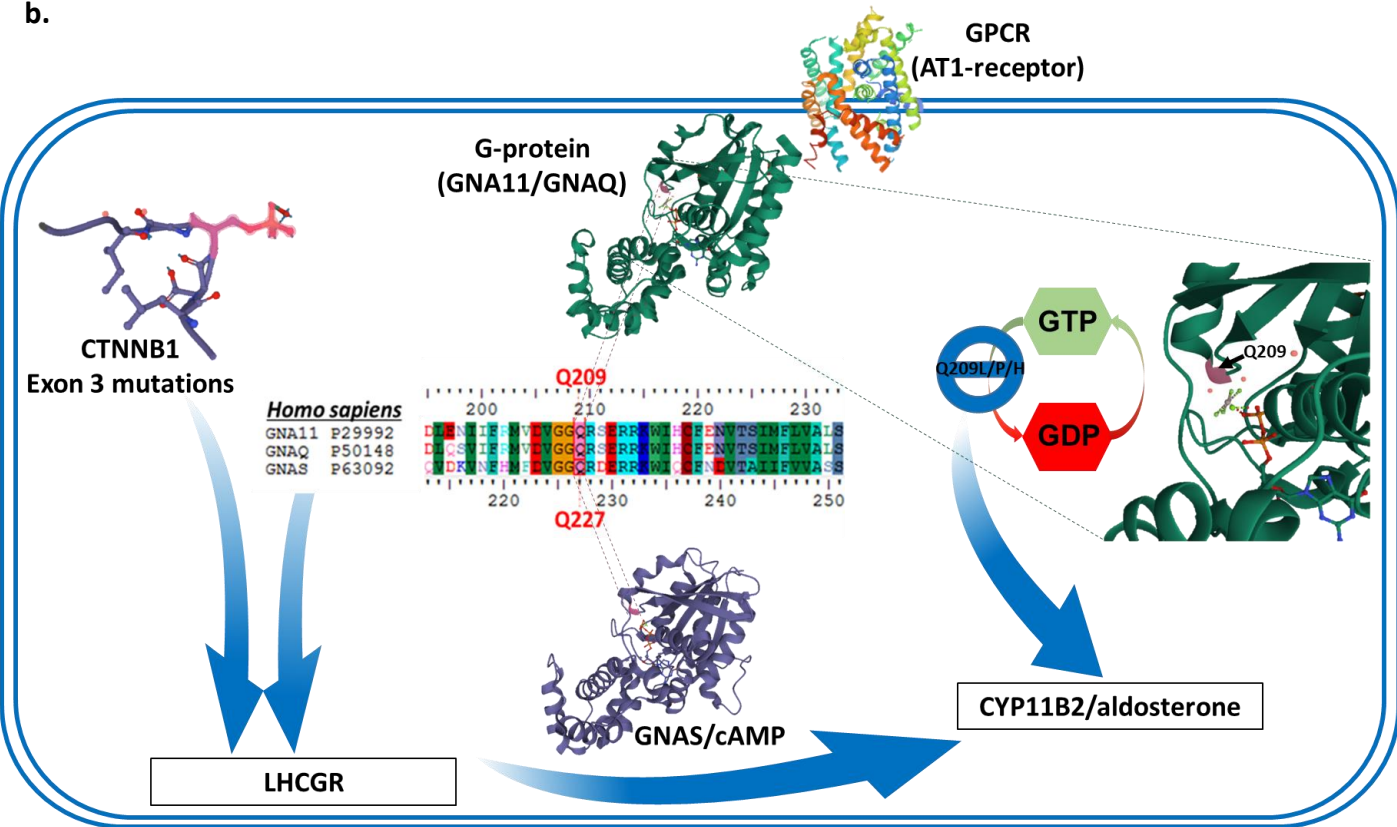


Figure 2 (a-f)

Mutations of *GNA11/Q* Q209 increase aldosterone production in human adrenocortical cells.

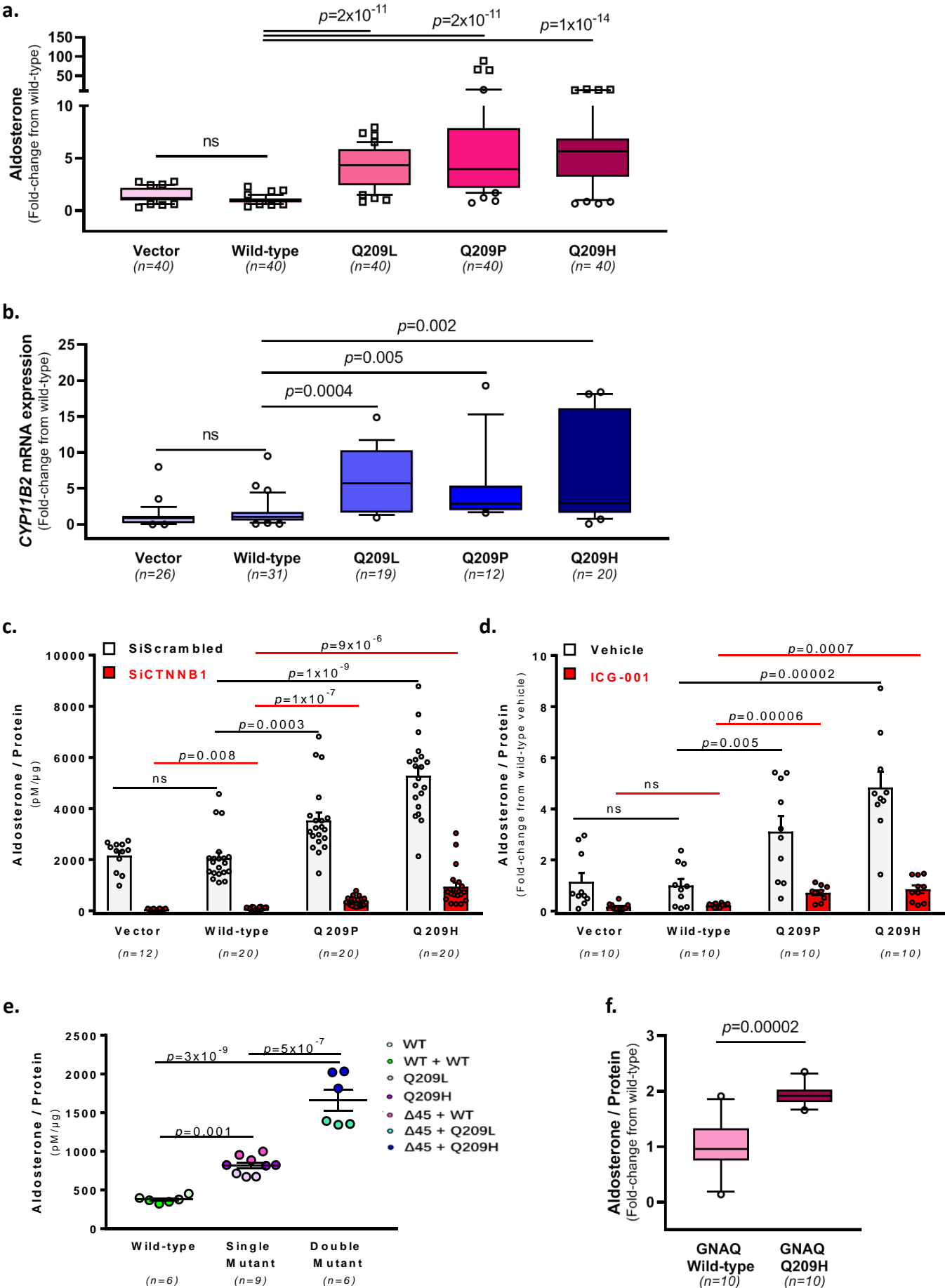
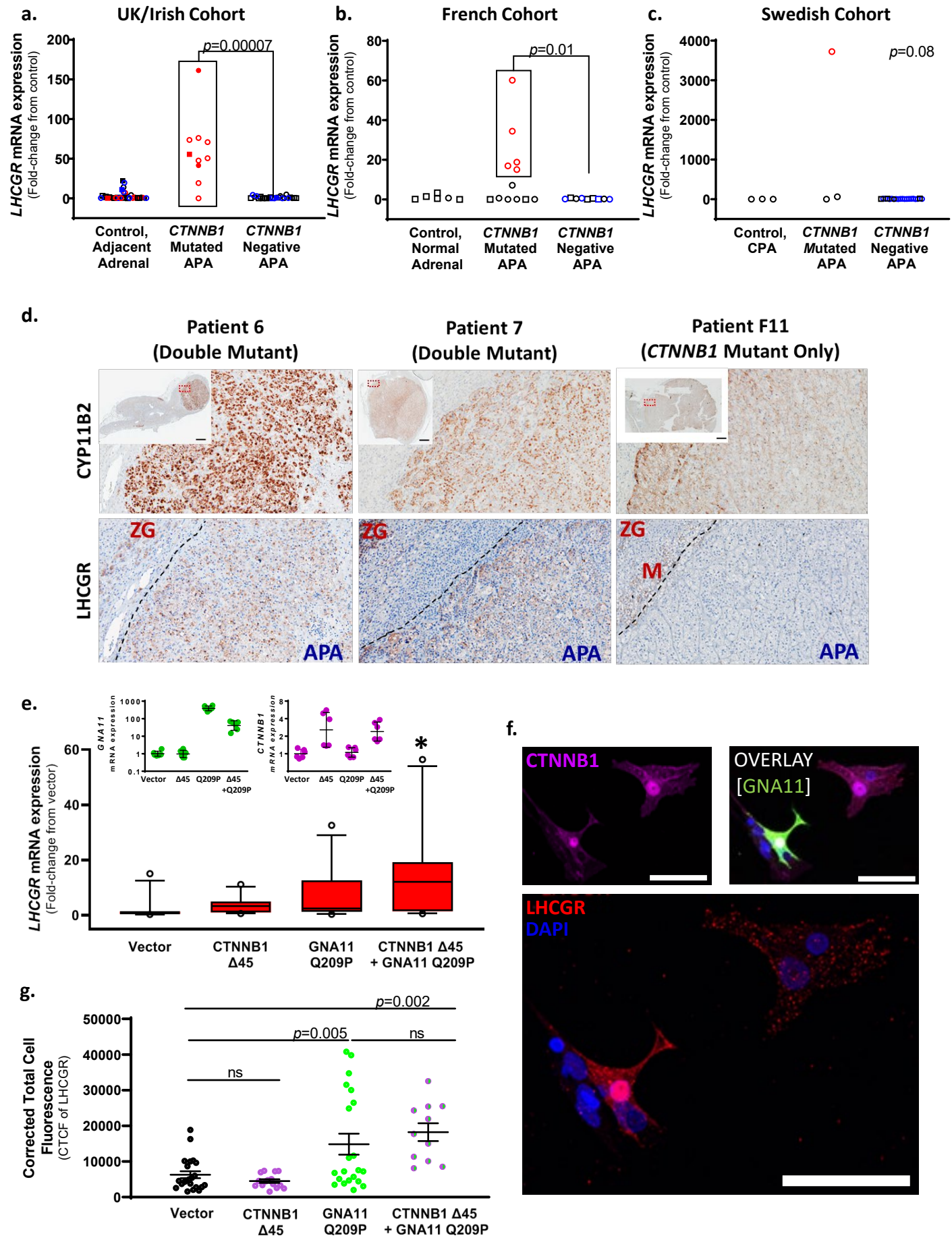


Figure 3 (a-g)

High LHCGR expression in *GNA11/Q* and *CTNNB1* double mutant aldosterone-producing adenomas (APAs) and double mutant co-transfected primary human adrenal cells.





**Figure 4 (a-f)**  
Gene expression profiles in *GNA11/Q* and *CTNNB1* double mutant adrenal cells.

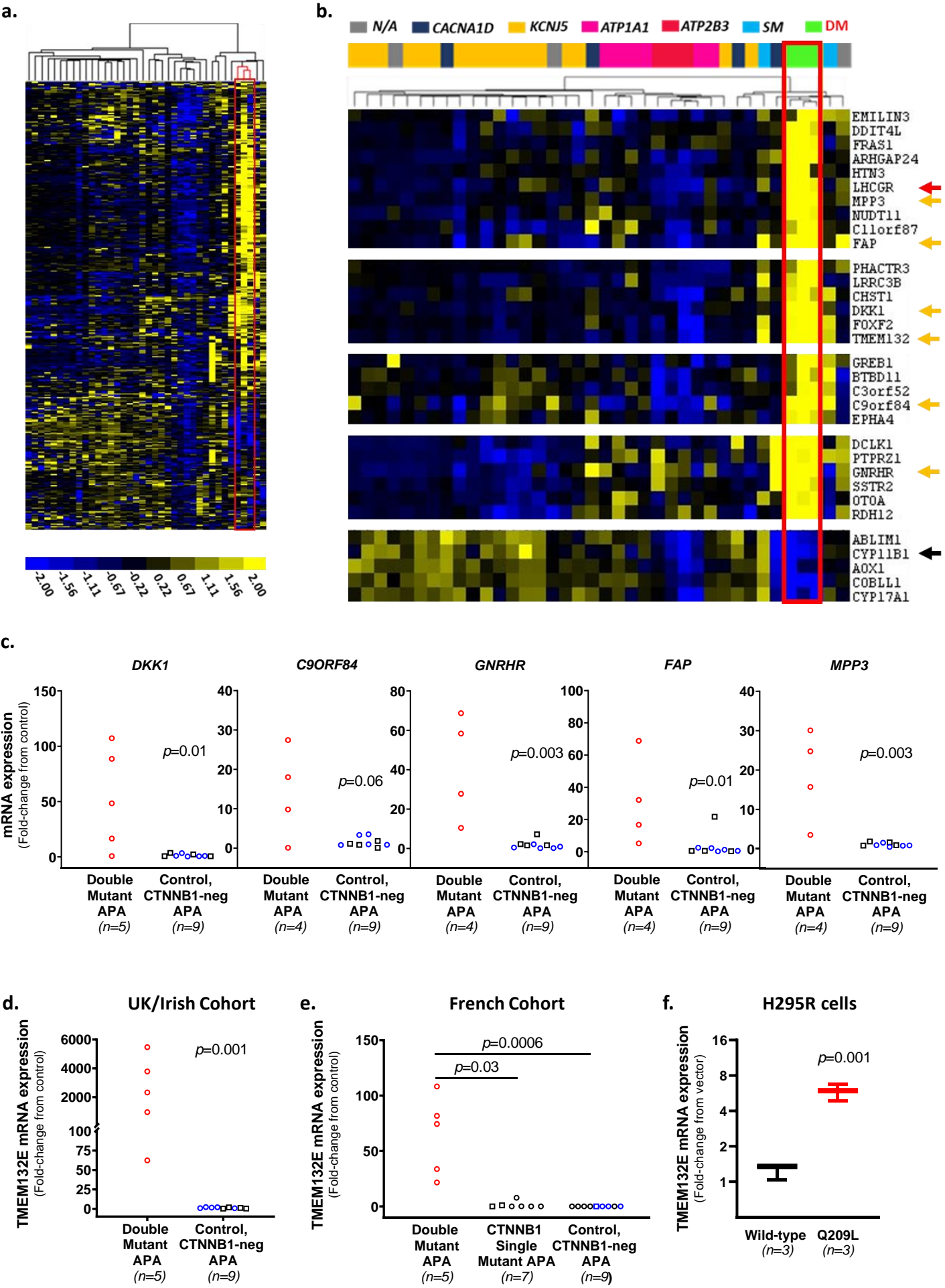
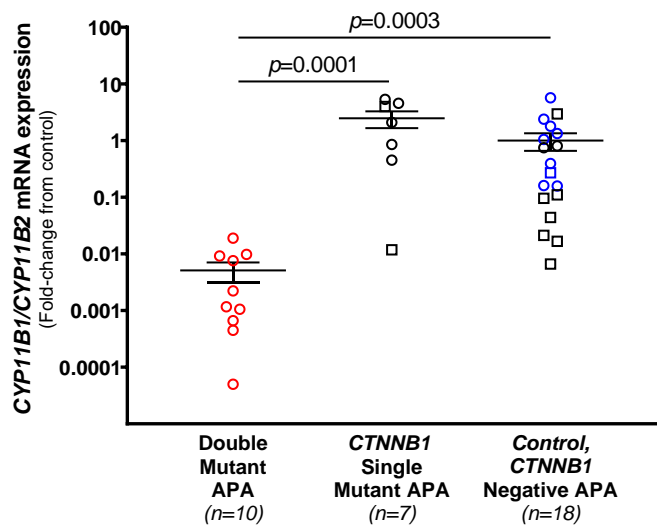




Figure 5 (a-b)

Aldosterone synthase (CYP11B2) and 11 $\beta$ -hydroxylase (CYP11B1) expression in *GNA11/Q* and *CTNNB1* double mutant APAs.

a.



b.

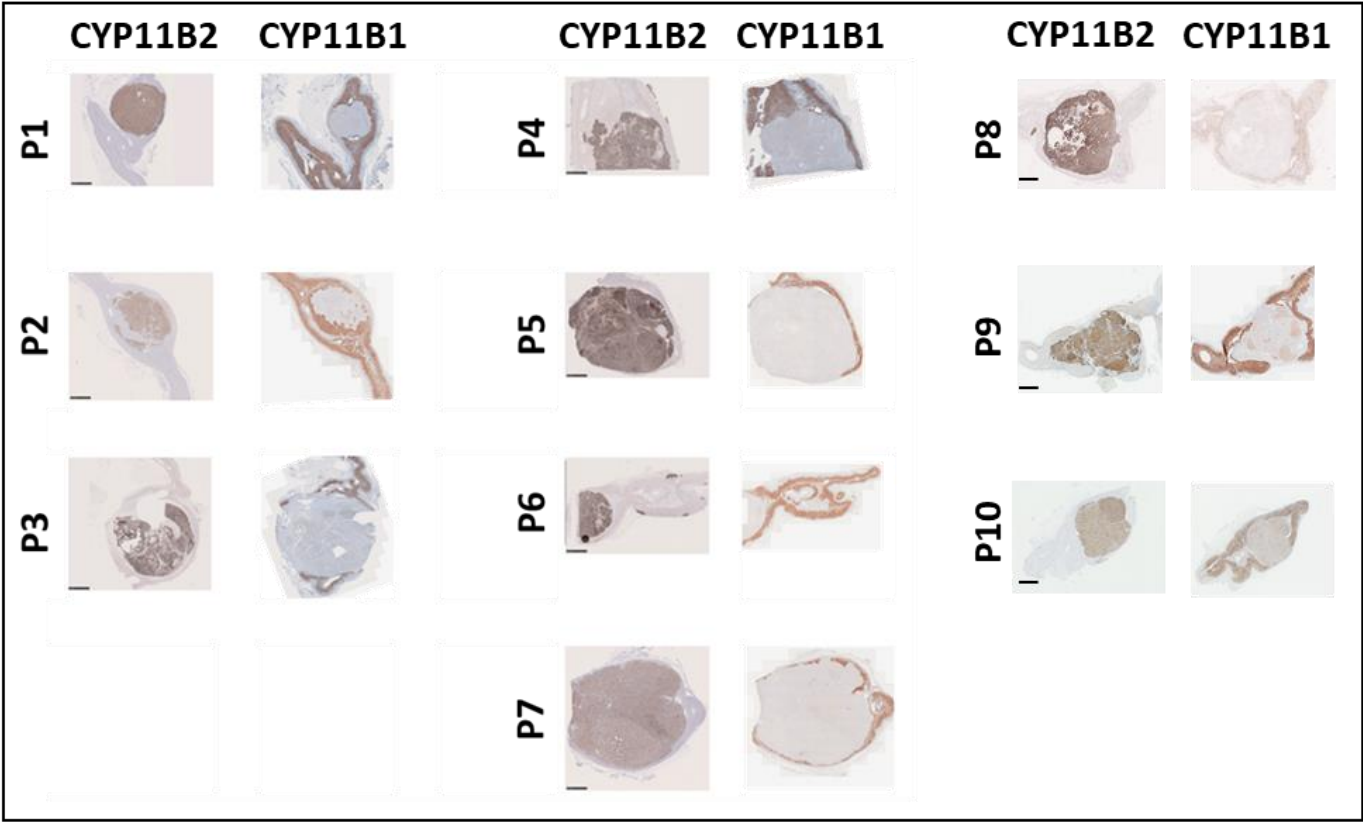
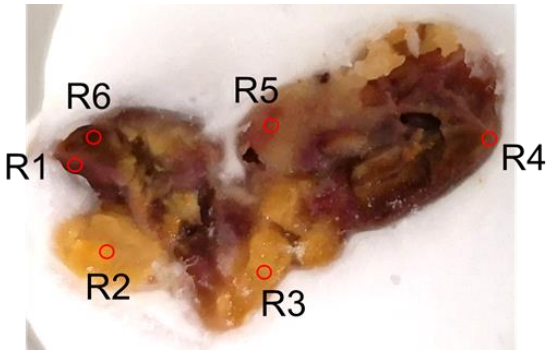


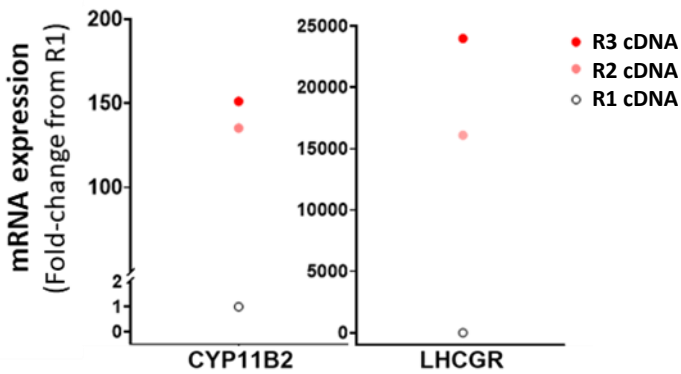
Figure 6 (a-f)

*GNA11* somatic mutations were found in the adjacent adrenals to double mutant APAs of Patient 7 (a-c) and Patient 1 (d-f).

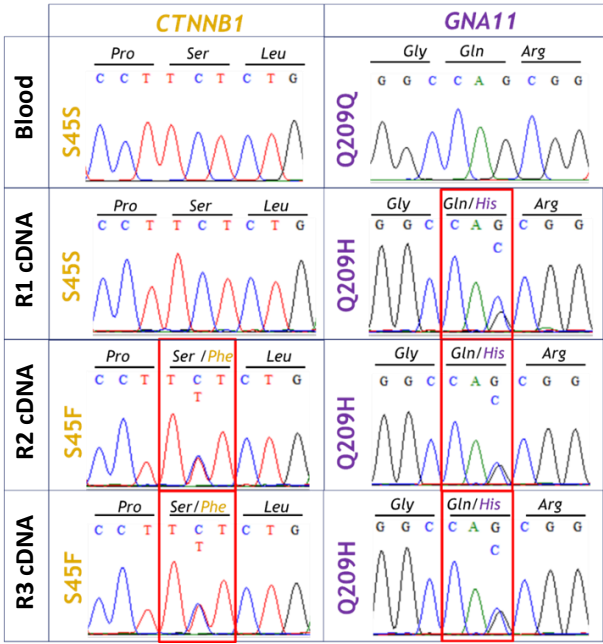
a.



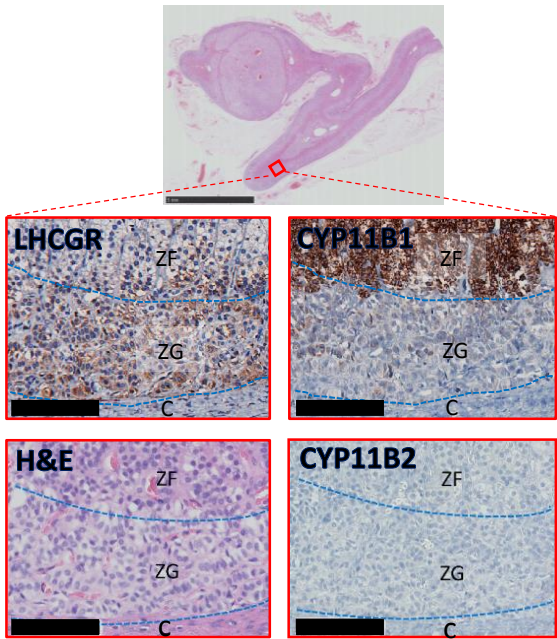
b.



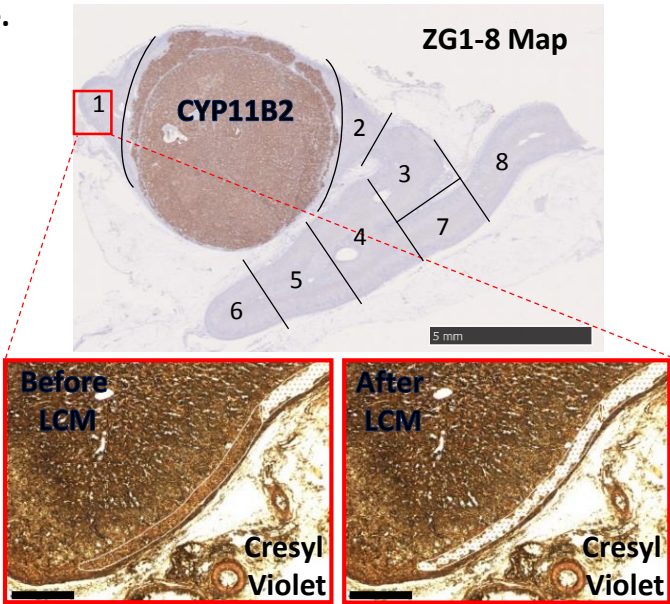
c.



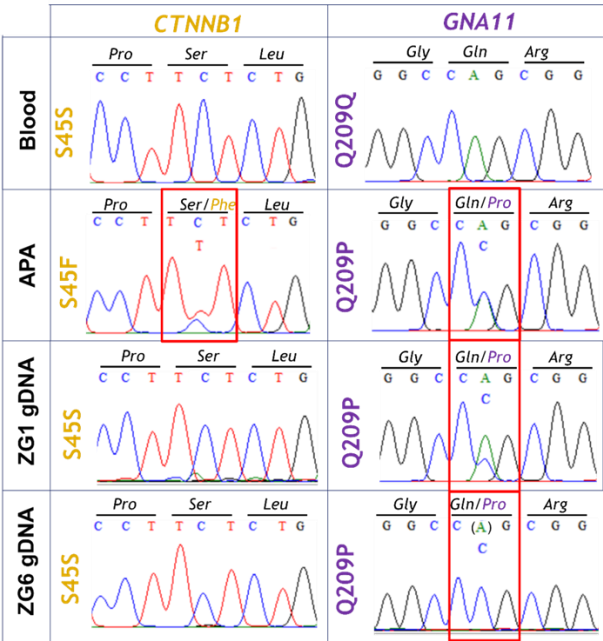
d.



e.



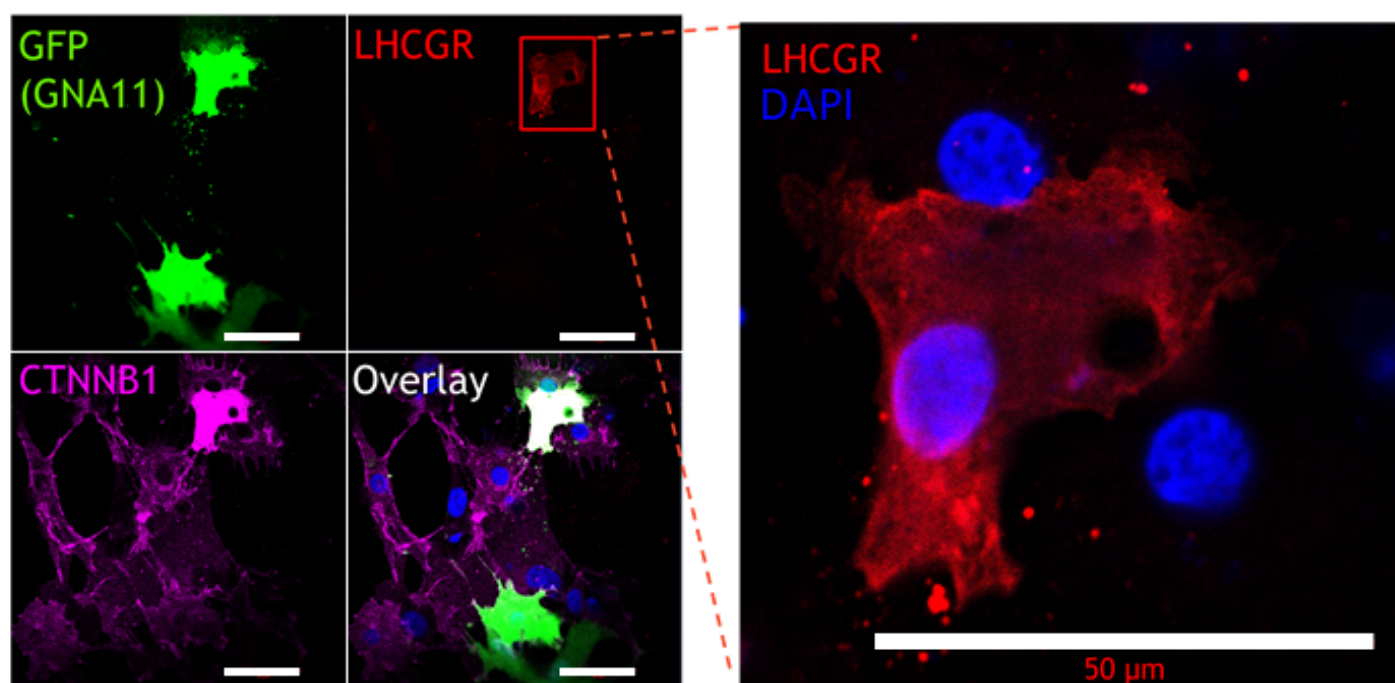
f.



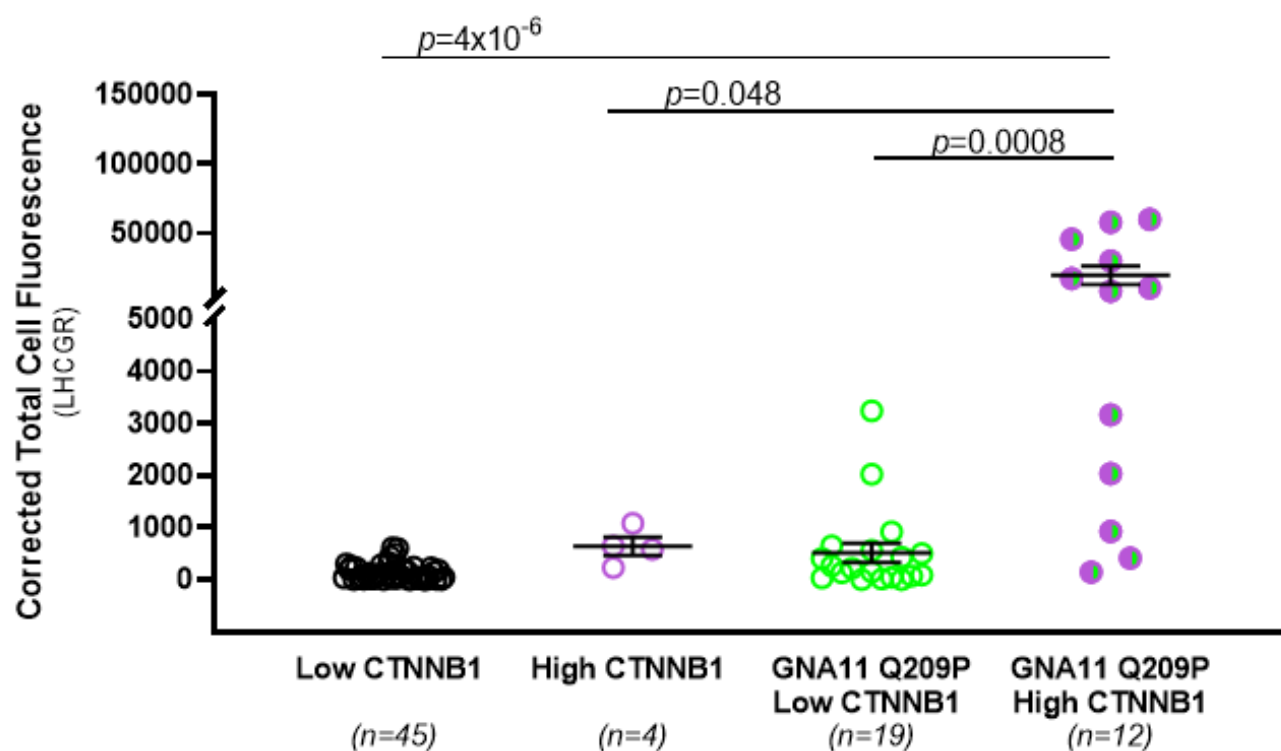
# Extended Data Figure 1 (a-b)

APA 351T cells transfected with *CTNNB1* (untagged plasmid) and *GNA11* (GFP tagged plasmid) wild-type or Q209P.

a.



b.



# Extended Data Figure 2 (a-d)

*GNA11* somatic mutations were found in the adjacent adrenal to double mutant APA of Patient 6.

